VATNAJÖKULL:
Mass balance, meltwater drainage and surface velocity of the glacial year 2018_19

Institute of Earth Sciences
University of Iceland
and
National Power Company

Finnur Pálsson
Andri Gunnarsson
Gestur Jónsson
Hlynur Skagfjörð Pálsson
Sveinbjörn Steinþórsson

RH-01-20

Contents:

Figures:

1. **INTRODUCTION**

In 1992 (glacial year 1991_92) a program of surface mass balance measurements was started for Vatnajökull by the Science Institute University of Iceland (now Institute of Earth Sciences, IES) in collaboration with the National Power Company (NPC). For the first year the program was limited to the western part of the glacier, but then expanded to include the northern outlets as well. In 1996 this study was further expanded to include southern outlets, with support from The European Union (Framework IV - Environment and Climate, TEMBA project 1996-1997). This program was extended 1998–2000 with further support from EU (Framework IV - Environment and Climate, ICEMASS project, 1998-2000). In 2000-2002 NPC and IES continued the program. In 2003-2005 IES participated in a multinational research project, which was financially supported by The European Union (EVK2-CT-2002-00152 SPICE). IES was responsible for obtaining data sets for calibration of models of the mass balance and dynamics of Vatnajökull. This work was also supported by The National Power Company of Iceland and The National Road Authority, and was a continuation of the TEMBA-project of 1996-97 and ICEMASS project 1998-2001.
Since then IES and NPC have continued a similar program. Mass balance measurements on the southeast outlet Breiðamerkurjökull is financially supported by the National Road Authority.
The aim of the collaborative work of NPC and IES is to improve understanding of the mass balance and melt water runoff from glaciers. This work in combination with energy balance measurements by NPC and IES on Vatnajökull will is used for calibration of models of the surface energy and mass balance of Vatnajökull.
This report describes the field measurements, mass balance, melt water runoff and GPS survey, for the glaciological year 2018_19.

2. DIARY

March 3 - 5: installation of melt wires, maintenance of AWSs on Breiðamerkurjökull.
March 30 - May 6: measurements of the winter balance, setup of AWSs.
May 30 - June 8: measurements of the winter balance, setup of AWS on Bárðarbunga.
October 18 - 22 and October 27 - 29: summer balance measurements; take down of AWSs, maintenance of AWSs on Breiðamerkurjökull.

In all expeditions and short visits to the glacier the locations of mass balance stakes were measured with Kinematic GPS (or fast static GPS) for surface velocity calculation.

The following members of staff of the Institute of Earth Sciences, University of Iceland, carried out the fieldwork on Vatnajökull: Finnur Pálsson, Sveinbjörn Steinþórsson, Eyjólfur Magnússon with Andri Gunnarsson, Gestur Jónsson (National Power Company) and Hlynur Skagfjörð Pálsson (Reykjavík Rescue Team).
Members of the Iceland Glaciological Society participated in the June fieldwork.

3. MASS BALANCE MEASUREMENTS

The purpose of the mass balance measurements is to describe the temporal and spatial distribution of the components of the mass balance. The mean annual values of the components and their variation from year to year are analyzed and related to meteoro-logical conditions and climatic variability. The results are used in studies of changes in the glacier volume, estimates of meltwater contribution to glacial rivers, mass balance modeling, evaluation of altitudinal and regional variations of mass balance in response to climatic variations, and to assess the hydrometeorological and dynamic response of the ice cap to climate change.

The mass balance was determined by a stratigraphic method, measuring changes in thickness and density relative to the summer surface. The winter balance was estimated by drilling ice cores through the winter layer in the spring. Ablation was monitored from markers; snow stakes were put up on the glacier and wires were drilled down in the ablation area. The summer balance was measured in the autumn.

3.1 Methods

Measurements of the surface mass balance on a large ice cap like Vatnajökull are impractical in terms of cost with conventional techniques and sampling density that are typically used on small glaciers. The spatial variability of the mass balance may, however, be predictable on the flat large outlets of such an ice cap given data on several profiles extending over the elevation range of the glacier. The precipitation generally increases with elevation and decreases with the distance from the coast, but both the distribution of snowfall and redistribution of snow by drift depend on the prevailing wind direction during the winter. The summer melting depends mainly on the altitude and the albedo of the glacier surface. Therefore, we have used observations along a limited number of flowlines, which span the elevation ranges of the outlets to assess aerial estimates of surface mass balance. Each profile describes the variation with elevation, but together they also describe the lateral variation of the mass balance. Recently, modern over-snow vehicles and helicopters have allowed fast traverses to ensure successful fieldwork in spite of frequently poor weather conditions. The error for individual point measurement is estimated ~30 cm_{we} for both summer and winter balance. The error for the glacier wide specific mass balance, based on area integral of mass balance, is however considered smaller, since the error for individual survey sites is independent.

The winter mass balance (b_w) is defined as the mass of snow accumulated during the winter months, the summer balance (b_s) is the mass balance during the summer, and the net balance (b_n) is defined as their sum. The specific mass balance is expressed in terms of the equivalent thickness of water. All mass balance components apply to a time interval between given measurement dates, which are not fixed from one year to another. The dates in the autumn are separated by approximately one calendar year, which roughly coincides with the glaciological year defined as October 1st to September 30th. Snow cores are drilled in April-May through the winter layer and profiles of the density are measured. The summer balance is derived in the autumn from measurements of the changes in the snow core density during the summer in the accumulation area and from readings at stakes and wires drilled

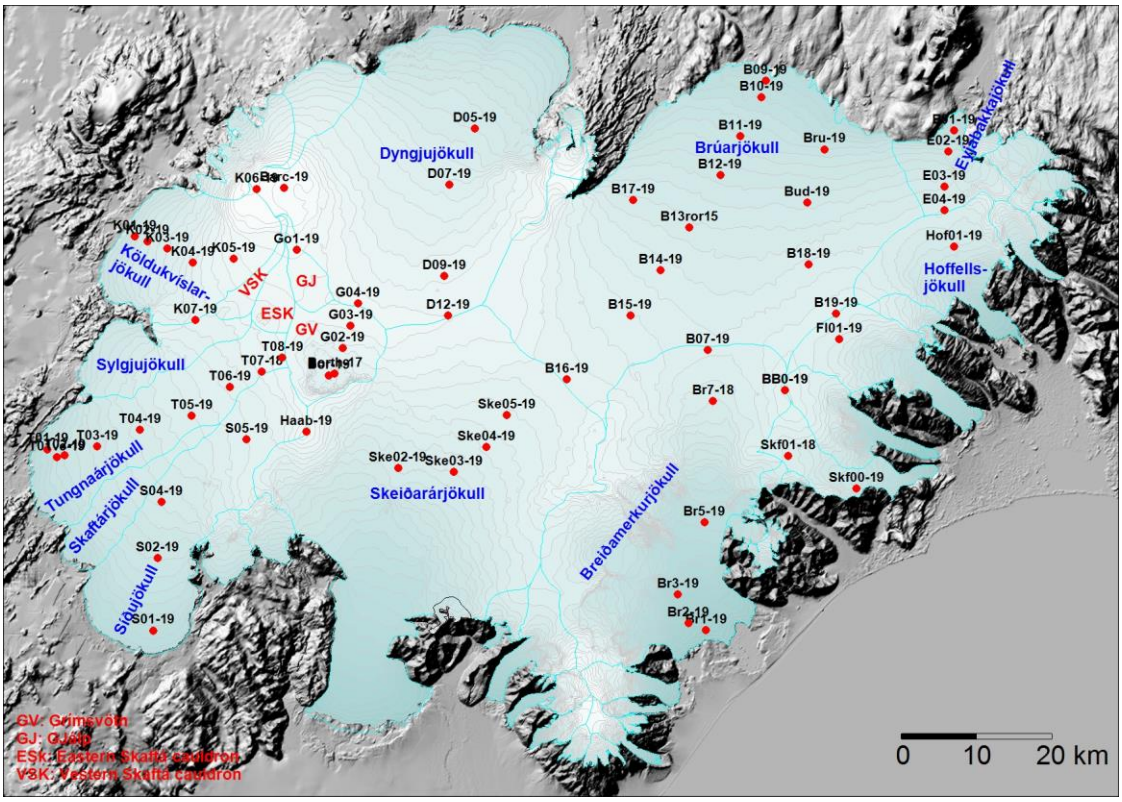

Figure 1. Outlets of Vatnajökull and location of mass balance survey sites 2018_19.

into the ice in the ablation areas.

Digital maps are created for winter, summer and net balance for the whole ice cap based on the in-situ measurements. The mass balance is calculated over both the ice and water drainage basins. The summer balance over the water basin is an estimate of meltwater contribution to rivers and groundwater storage. This estimate, however, does not include precipitation that falls as rain on the glacier or snow, which falls and melts during the summer. The meltwater contribution is compared with river runoff at stream flow gauges closest to the glacier. For this comparison, we define the glaciological year from the start of October to the end of September and the period draining meltwater from the glacier during the summer from start of June through September. It would be misleading to include May in the summer period because runoff from the glacier melt in May is delayed due to refreezing during the elimination of the frost in the surface layer.

3. 2 Results of mass balance measurements.

Mass balance measurements were done at 61 sites in spring 2019 (Fig. 1). The specific mass balance at individual sites is shown in Fig. 2. Most sites are on central flow lines at individual outlets. The specific mass balance along approximate flow lines is given in Fig 3. for the glacier outlets: Síðujökull, Tungnaárjökull, Köldukvíslarjökull, Dyngjujökull, Brúarjökull (west and east), Eyjabakkajökull, Breiðamerkurjökull, SE-Vatnajökull and the ice catchment of Grímsvötn.

Digital maps for winter, summer and net balance are shown in Figure 4. Although no balance measurements are available for Skeiðarárjökull, the balance has been estimated by interpolating the balance values from the neighboring outlets, based on our experience from previous years. The mass balance of individual outlet is discussed in the following subsections.

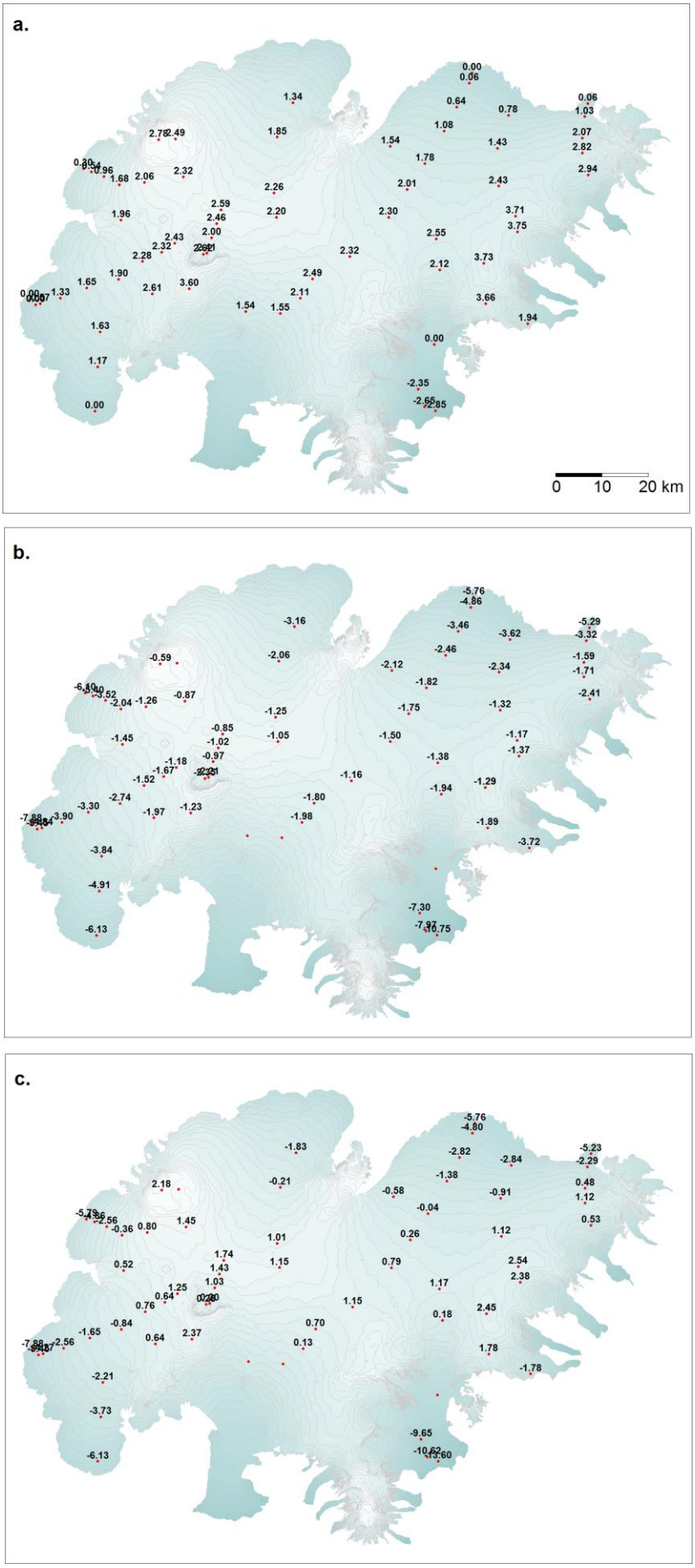

Figure 2. Maps showing point values of specific surface mass balance in m water equivalent (m_{we}), 2018_19. a. winter, b. summer, c. net balance.

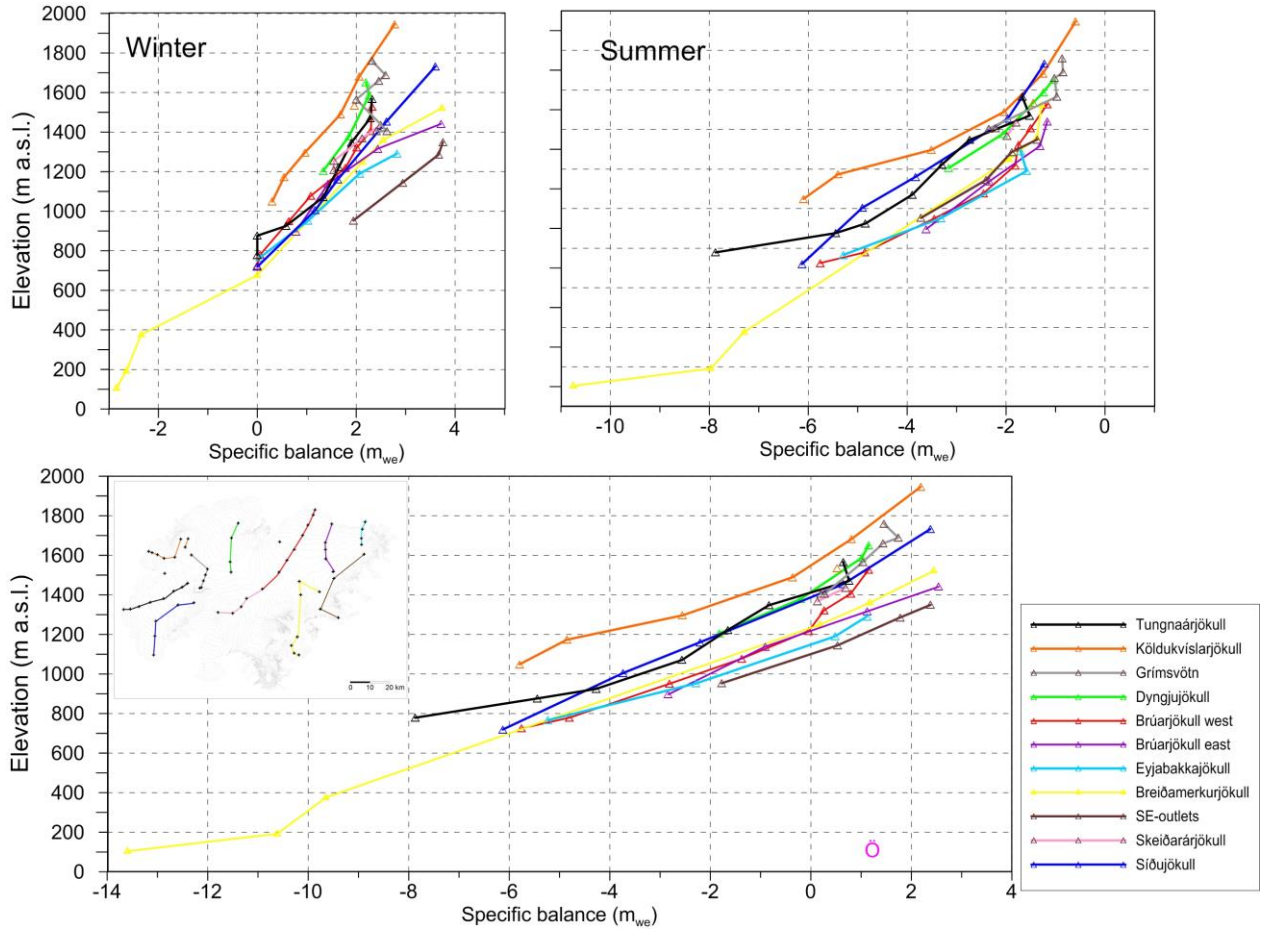

Figure 3. a. Specific point mass balance (m_{we}), along all mass balance profiles 2018_19.

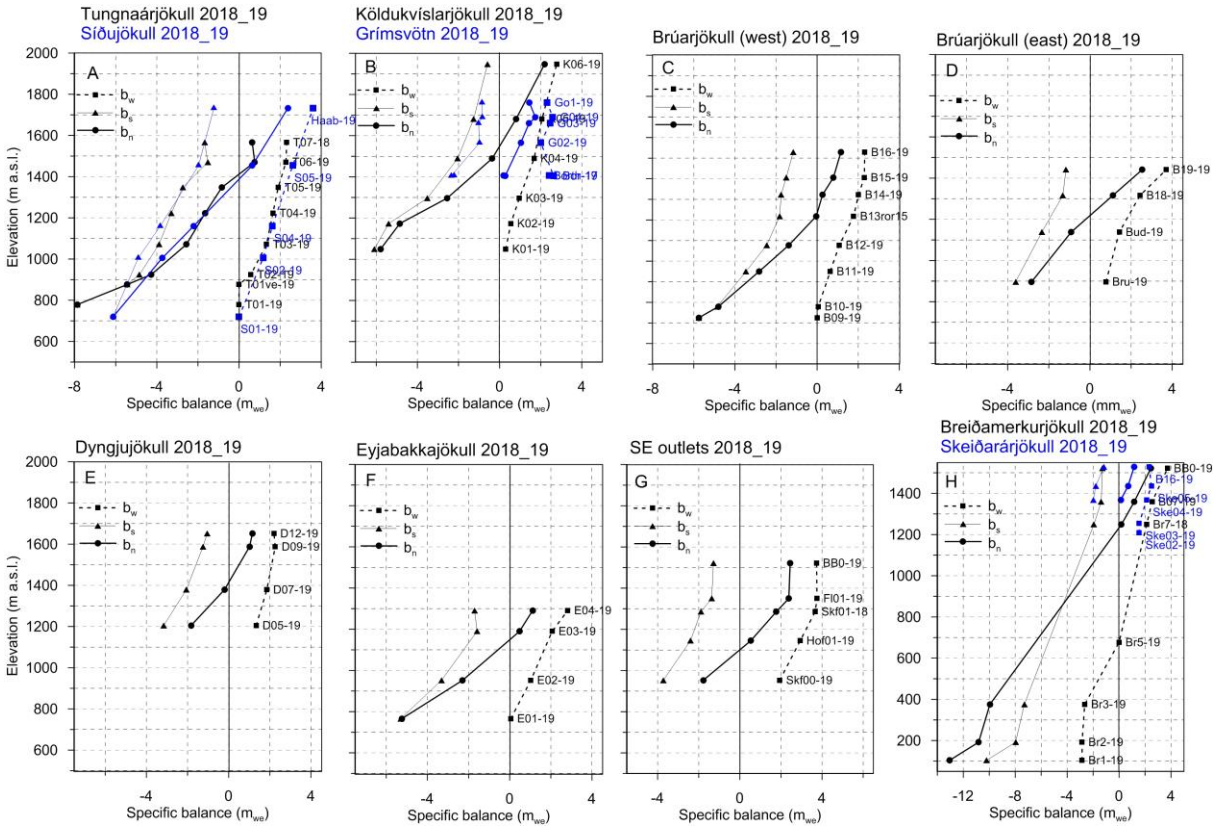

Figure 3. b. Specific point mass balance (m_{we}) 2018_19 as a function of elevation on central flow lines on Vatnajökull outlets.

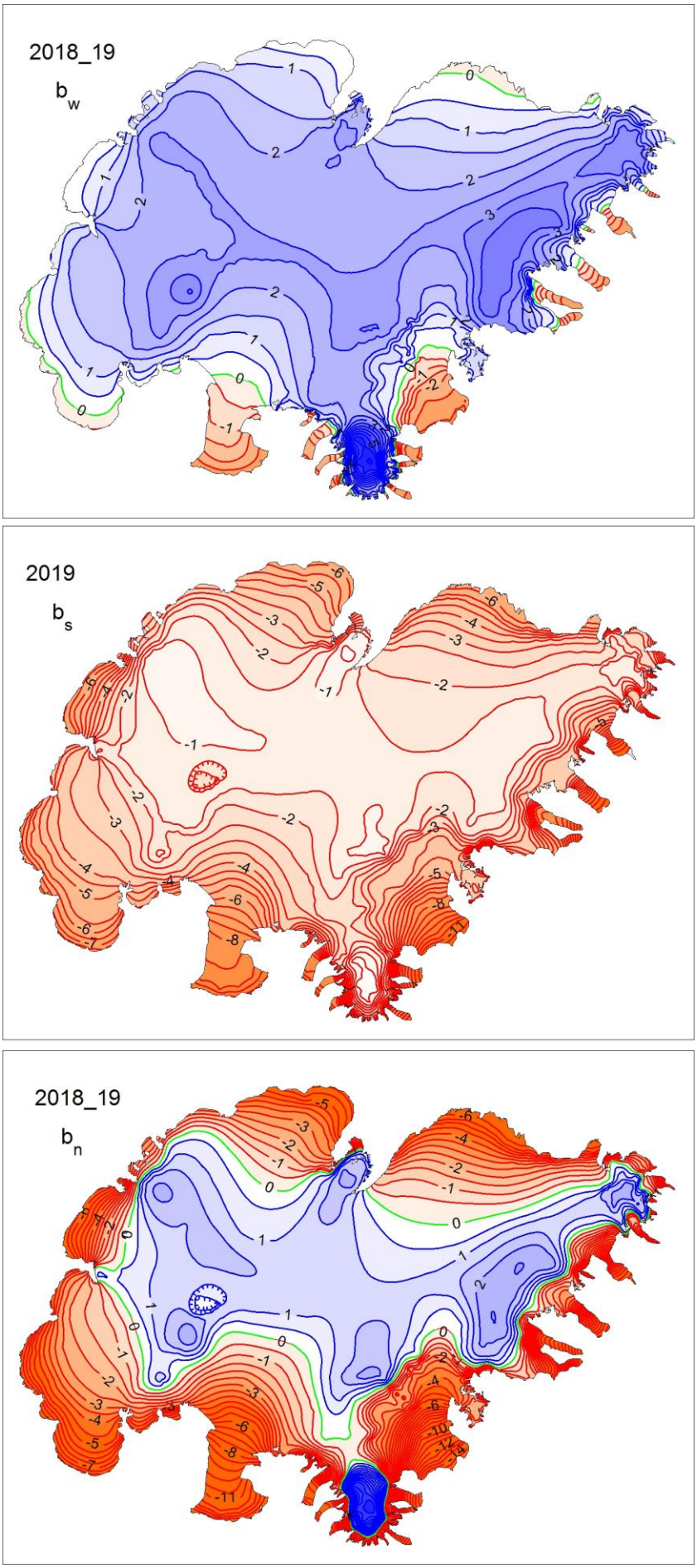

Figure 4. Specific mass balance (m_{we}) maps of Vatnajökull 2018_19. Top: winter, Centre: summer, Bottom: net balance.

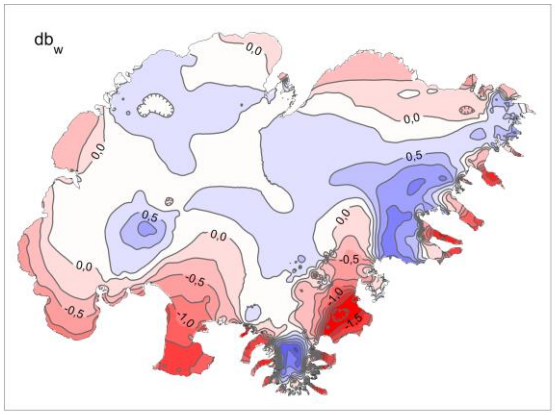

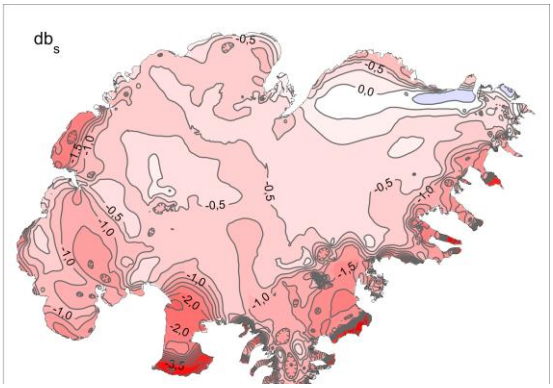

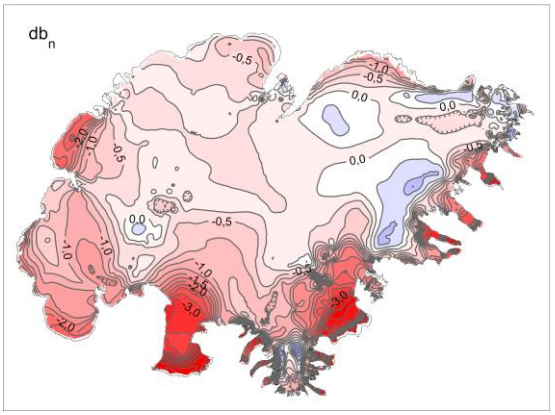

Figure 5. Top left: The difference between winter balance in 2018_19 and the average winter balance 1995_96 to 2017_18. Top right: The difference between summer balance in 2018 and the average summer balance 1996 to 2018. Lower left: The difference between net balance in 2018_19 and the average net balance 1995_96 to 2017_18. (Blue is higher than average balance and red lower than average).

A surface DEM is needed for surface area distribution and delineation of ice divides for individual outlets and catchments. The currently used surface DEM is mostly based on SPOT5 satellite images in 2010*, and partly from LiDAR survey 2010 -11 and -12 (**Jóhannesson et al. 2013), but the large set of GPS profiles measured in spring 2015 was used to locally shift the older DEMs. This DEM representing the surface of 2015 but now cut to the glacier terminus of 2017, of was used in all area distributions; ice and water divides were not reworked.

The weather in the autumn and first winter months 2018-19, was wet and rather warm, not much snow below ~1000 m. February and May were also relatively warm with more than average precipitation. The spring was relatively cold and dry.

Figure 5 (top left) shows that the winter accumulation is over average at all higher accumulation zones, but less than average in all the ablation zones. Winter melting at the low lying S-outlets was more than average.

The summer months were mostly warm and dry in the west but mid summer had prevailing high winds from NE to E direction with overcast in the east. The extremely thin winter snow cover in the highlands melted in early spring and the dry weather allowed for surface dust to be airborne and precipitated on the glacier surface. This greatly lowered the surface albedo and enhanced melt. The dust in the summer surface of the accumulation zone was in higher quantity than noticed before during the survey period. Samples were taken at selected sites and will be analyzed.

*SPOT 5 HRG images were made available by the French Space Agency (CNES) through the ISIS (Incentive for the Scientific use of Images from the SPOT system) program and SPOT 5 HRS digital elevation models by the Spot Image project Planet Action (www.planet-action.org) and the SPIRIT SPOT 5 stereoscopic survey of Polar Ice.

**Jóhannesson, T., Björnsson, H., Magnússon, E., Guðmundsson, S.,Pálsson, F., Sigurðsson, O., Thorsteinsson, T., and Berthier, E.: Ice-volume changes, bias estimation of mass-balance measurements and changes in subglacial lakes derived by lidar mapping of the surface Icelandic glaciers, Ann. Glaciol., 54, 63–74, doi:10.3189/2013AoG63A422,2013.

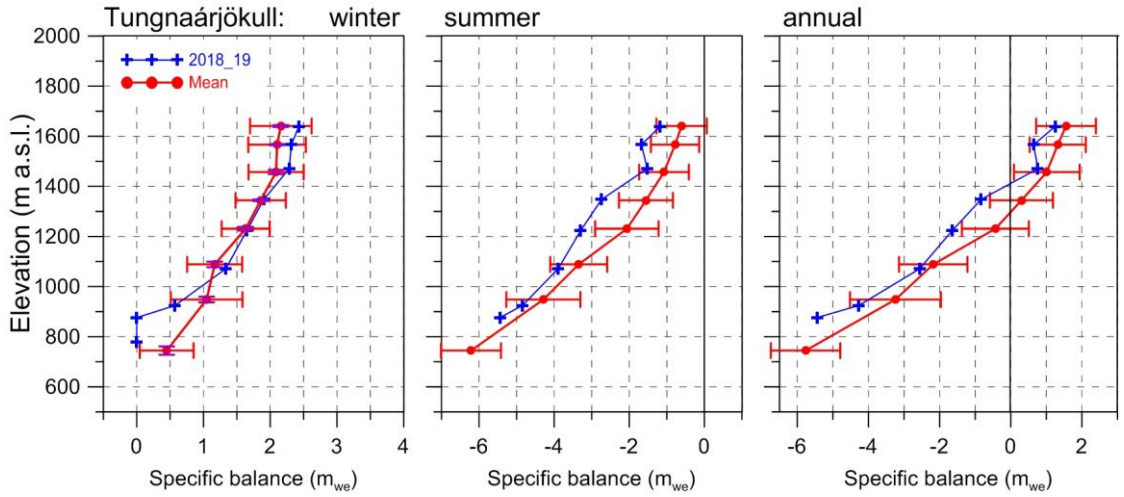

Figure 6. Mass balance at a central flow line of Tungnaárjökull 2018_19 and average mass balance 1991_92 to 2018_19 (the horizontal red lines indicate st. dev of the variability at the survey site during the survey period),

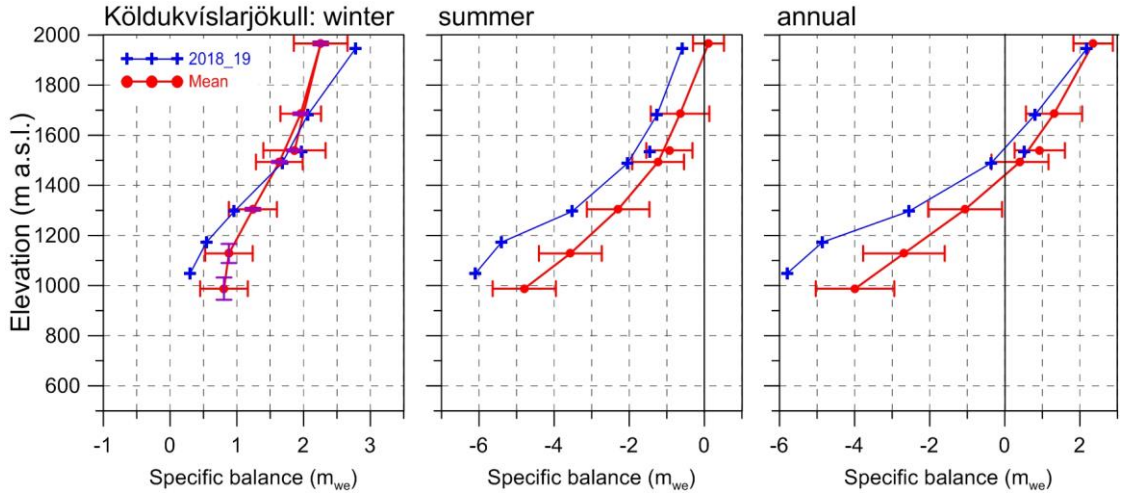

Figure 7. Mass balance at a central flow line of Köldukvíslarjökull 2018_19 and average mass balance 1991_92 to 2018_19.

3.2.1 Tungnaárjökull.

Area = 332 km^2
B_w= 0,49 km^3_{we} ; b_w = 1,49 m_{we}
B_s = -1,13 km^3_{we} ; b_s = -3,40 m_{we}
B_n = -0,64 km^3_{we} ; b_n = -1,91 m_{we}
ELA = 1415 m a.s.l. (at profile)
AAR = 25 %
(The terms are defined at the foot of this page)

Variation of mass balance along a central flow line on Tungnaárjökull is shown in Fig. 6. The winter accumulation was over average at the highest survey sites and but far less at lowest. The total winter balance was almost at average (98%). Summer mass loss was ~1 std. over average at survey sites in the accumulation zone, but ~average in the ablation zone. Summer mass loss was 30% more than average of the survey period. Similar applies to the net balance. In total the net mass loss was 76% more than average of the survey period. This is the 25th year out of the 28 surveyed with negative net balance.

3.2.2 Köldukvíslarjökull

Area = 289 km^2
B_w = 0,41 km^3_{we} ; b_w = 1,41 m_{we}
B_s = -0,84 km^3_{we}; b_s = -2,92 m_{we}
B_n = -0,43 km^3_{we}; b_n = -1,51 m_{we}
ELA = 1550 m a.s.l. (at profile)
AAR = 38 %

Variation of mass balance along a

For each ice catchment basin, B_w, B_s and B_n are water equivalent volumes of winter, summer and net balance, ELA the equilibrium line altitude, and AAR is the accumulation area ratio.

central flow line on Köldukvíslarjökull is shown in Fig. 7. The winter accumulation was more than average at highest and under average at lowest survey sites, by ~1 std.. The total winter balance was 5% above average. Summer mass loss was 1-2 std. over average at all survey sites and in total 52% over average during the survey period. Similar applies to the net balance, except at the highest site where high winter accumulation and high summer mass loss balance out. In total the net mass loss was 3-fold that of an average year of the survey period. This is the 25th year out of the 28 surveyed with negative net balance.

3.2.3 Dyngjujökull

Area = 1038 km^2
B_w = 1,90 km^3_{we} ; b_w= 1,83 m_{we}
B_s = -2,29 km^3_{we} ; b_s = -2,21 m_{we}
B_n = 0,39 km^3_{we} ; b_n = -0,38 m_{we}
ELA = 1415 m a.s.l. (at profile)
AAR = 59 %

Variation of mass balance along a flow line on Dyngjujökull is shown on Fig. 8. Mass balance is not measured at the lowest elevations, but assumed to be correlated (as a function of elevation) to that of Brúarjökull and Köldukvíslarjökull. Inspection of the winter Modis satillite images suggest that, at the glacier snout, snow cover was very thin below ~1000 m. The site measurements show over average snow accumulation in the accumulation zone (above 1200 m a.s.l.). The total winter accumulation is estimated 15% over the average of the survey period.
Summer mass loss was ~1 std. more than average over the survey period, at the survey sites. The mass loss was ~37% more than that of an average summer.
The total net balance was -0,38 m_{we} while the average for Dyngjujökull is only slightly negative (-0,02 m_{we}).
Dyngjujökull has often had mass balance close to zero, and the net balance has been estimated slightly positive in at least 6 years of the almost three decade period of almost continuous mass loss for Vatnajökull as a whole.

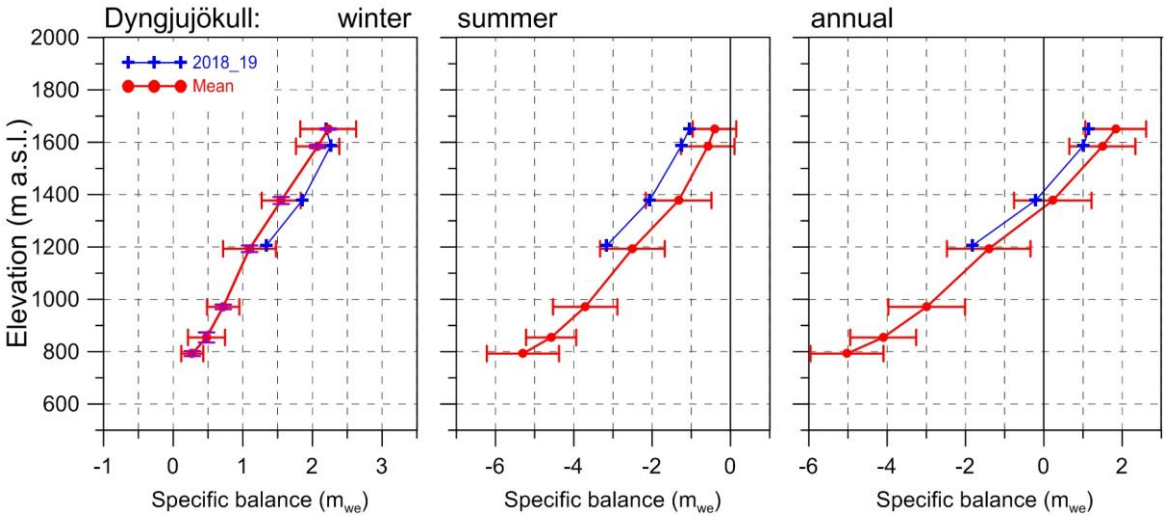

Figure 8. Mass balance at a central flow line on Dyngjujökull 2018_19 and average mass balance 1991_92 to 2018_19 (except 1998_99 – 2003_04 at all but the top elevation).

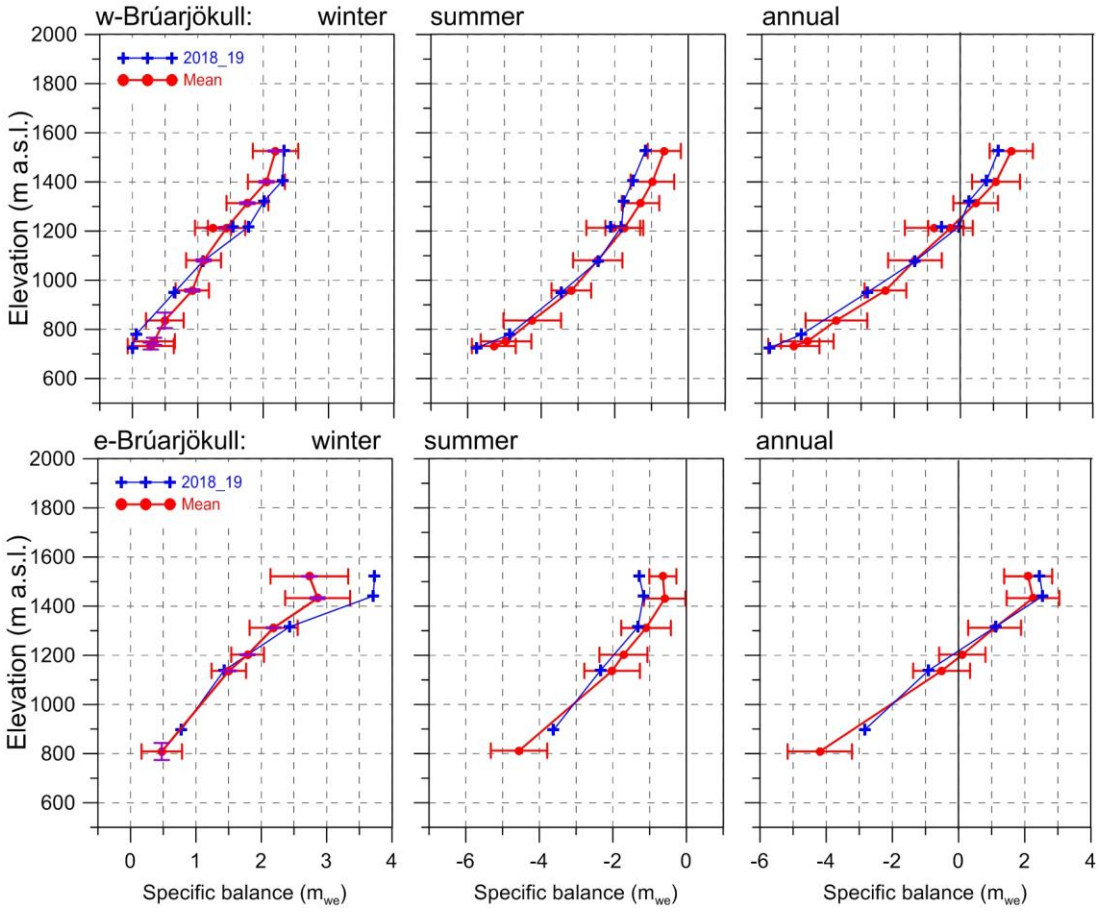

Figure 9. Mass balance at two flow lines on Brúarjökull 2018_19 and average mass balance 1992_93 to 2018_19.

3.2.4 Brúarjökull

Area = 1500 km^2
B_w = 2,75 km^3_{we} ;b_w = 1,84 m_{we}
B_s = -3,21 km^3_{we}; b_s = -2,14 m_{we}
B_n = -0,46 km^3_{we}; b_n = -0,30 m_{we}
ELA = 1220 m a.s.l. (western flow line)
ELA = 1210 m a.s.l. (eastern flow line)
AAR = 57 %

Variation of mass balance along two flow lines on Brúarjökull is shown on Fig. 9. In the upper accumulation zone winter snow was high over average with clear increasing trend towards east, with almost 1,5 std. higher than average accumulation at Breiðabunga, which is most prone to precipitation from eastern wind directions. In the ablation zone snow collection was close to average at most survey sites. The winter balance was about 15% higher than average during the survey period. Summer mass loss was close to average in the ablation zone but almost 1 std. more than average in the accumulation zone. Here, as in other regions of the accumulation zone of Vatnajökull, dirt in the surface enhanced melt. Some dirt was already blown onto the surface, from the early snow free highland, in the first weeks of summer. In total the mass loss in summer exceeded the average by 13%. The net balance was close to average at most sites. In total the net balance was negative by -0.30 m_{we}, not significantly different from the average of the survey period.
During the survey period, there have been 8 years of positive balance and 19 years with negative.

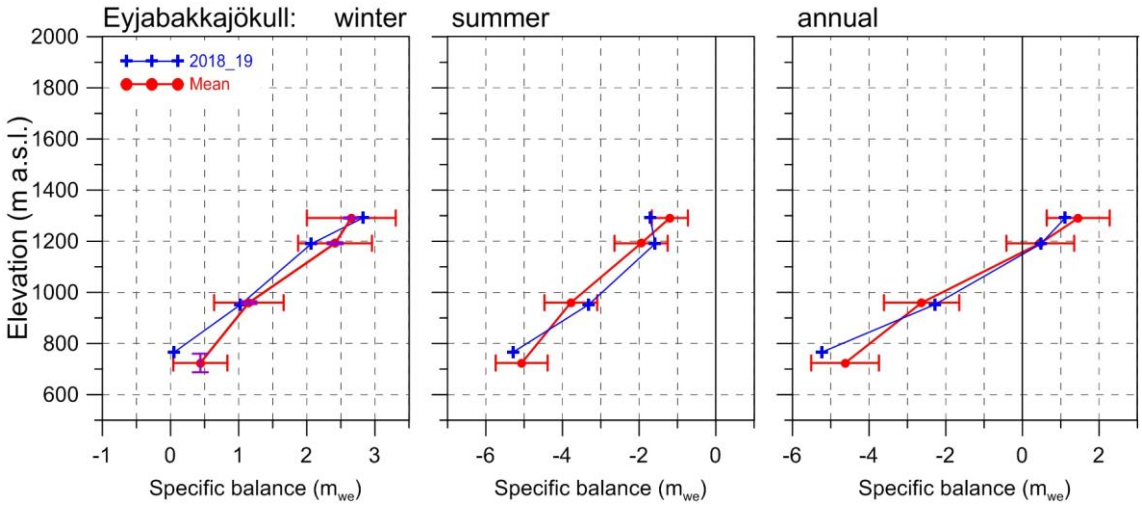

Figure 10. Mass balance at a central flow line of Eyjabakkajökull 2018_19 and average mass balance 1995_96 to 2018_19.

3.2.5 Eyjabakkajökull

Area = 108 km^2
B_w= 0,20 km^3 $_{we}$; b_w = 2,09 m_{we}
B_s = -0,28 km^3 $_{we}$; b_s = -2,48 m_{we}
B_n = -0,08 km^3 $_{we}$; b_n = -0,39 m_{we}
ELA = 1140 m a.s.l. (at profile)
AAR = 40 %

Variation of mass balance along a central flow line on Eyjabakkajökull is shown on Fig. 10. Accumulation was close to average at the higher sites, but up to 1 std. less than average at the lowest site reflecting the mostly warm winter. The total winter balance was at average of the survey period. Summer mass loss was less than average, caused by the cold and wet summer in the region; the net loss was ~95% of average. The net balance was negative by ~85% of the average since of the survey period.

3.2.6 Breiðamerkurjökull

Area = 925 km^2
B_w = 1,25 km^3 $_{we}$; b_w = 1,36 m_{we}
B_s = -3,18 km^3 $_{we}$; b_s = -3,44 m_{we}
B_n = -1,93 km^3 $_{we}$; b_n= -2,08 m_{we}
ELA = 1230 m a.s.l. (at profile)
AAR = 44 %

Variation of mass balance along a central flow line on Breiðamerkurjökull is shown on Fig. 11.
Winter accumulation was well over average at the highest survey sites in the accumulation zone. At the sites in

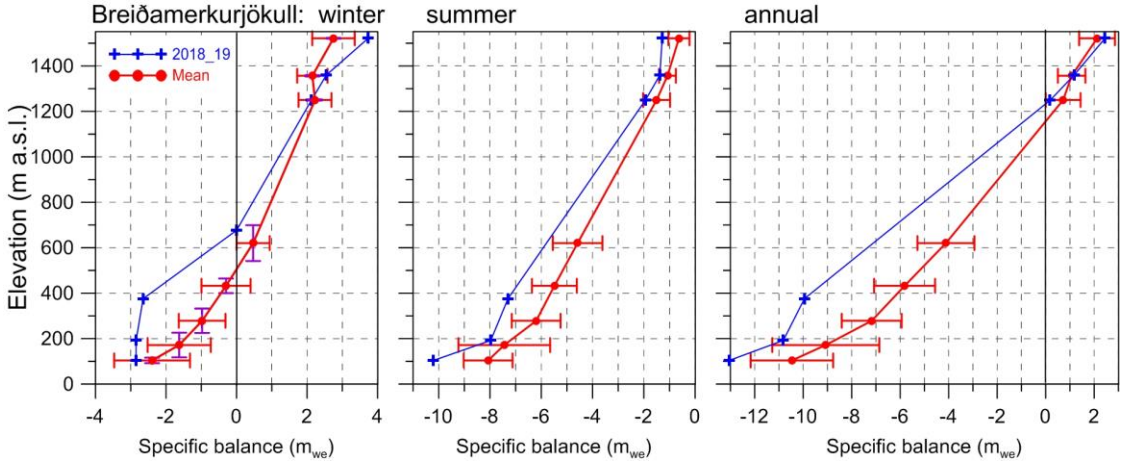

Figure 11. Mass balance at a central flow line of Breiðamerkurjökull 2018_10 and averaae mass balance 1995 96 to 2019 19.

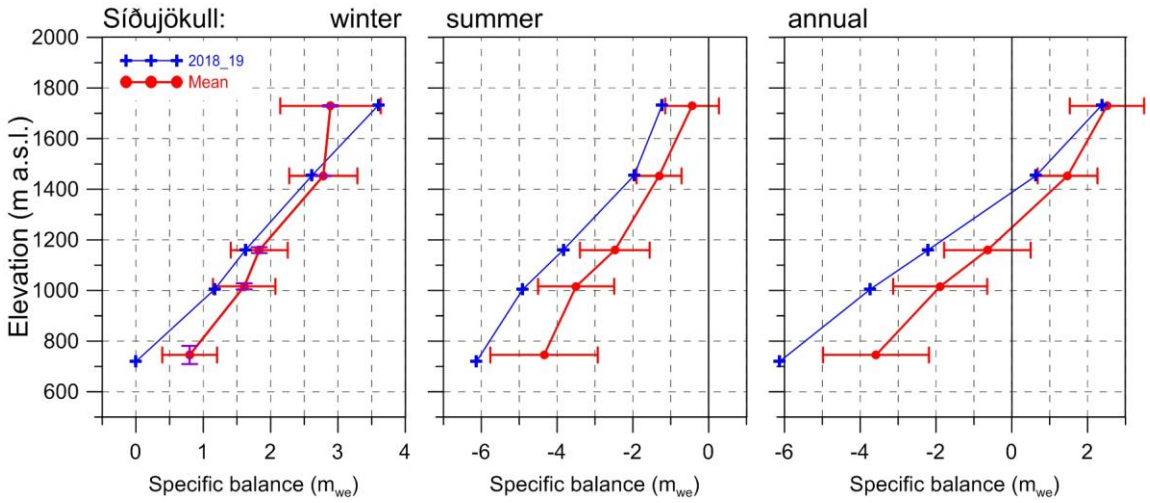

Figure 12. Mass balance at a central flow line of Síðujökull 2018_19 and average mass balance 2004_05 to 2018_19.

in the ablation zone, mass loss in winter was 2std. more than average at sites between 400 m a.s.l. but of ~50 m a.s.l.; most of this melt caused by the higher than average heat fluxes during the warm and windy winter. The total winter balance was ~90% of the average. Summer mass loss was ~1std. over average at all survey sites. The total summer mass loss was close to 35% more than average during the survey period. The net mass loss was almost two-fold that of an average year.

In addition to mass loss due to surface melt Breiðamerkurjökull loses in the order of 0,5 km^3 annually via calving into the marginal lake Jökulsárlón; this mass loss is not accounted for here.

3.2.7 Síðujökull

Area = 412 km^2
B_w= 0,61 km^3_{we}; b_w = 1,49 m_{we}
B_s = -1,57 km^3_{we}; b_s = -3,80m_{we}
B_n = -0,95 km^3_{we}; b_n= -2,32 m_{we}
ELA = 1390 m a.s.l. (at profile)
AAR = 28 %

Variation of mass balance along a central flow line on Síðujökull is shown in Fig. 12. Snow accumulation was ~1 std. more than average at the highest site but up to ~1.5 std. less than

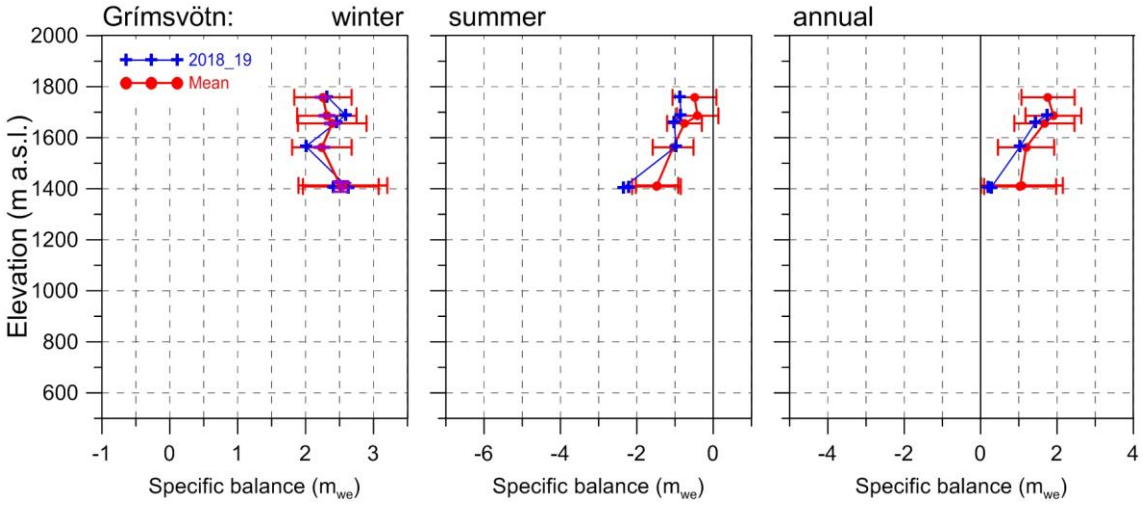

Figure 13. Mass balance at a flow line towards Grímsvötn 2018_19 and average mass balance 1991_92 to 2018_19.

average at the lower sites.
The total winter balance was ~92% of the average (since 2004_05). Summer mass loss was about 1 std. more than average at all sites, and the total summer mass loss was ~33% more than the average of the survey period. The net balance was at average at the highest site, but up to 1.5 std. more negative at the other sites. Net mass loss was 85% more than average.

3.2.6 Grímsvötn-Gjálp

Area = 174 km^2
B_w = 0,43 km^3_{we}; b_w = 2,50 m_{we}
B_s = -0,21 km^3_{we}; b_s = -1,33 m_{we}
B_n = 0,22 km^3_{we}; b_n= 1,17 m_{we}

Variation of mass balance at sites close to a flow line from Bárðarbunga towards Grímsvötn center is shown in Fig. 13. Snow accumulation was close to average at all survey sites, and total winter accumulation ~7% over the average. Summer mass loss was among the highest of the survey period, 66% over the average. Net balance was positive but only 75% of the average. In addition to surface mass loss in summer geothermal melt in the Grímsvötn area is on the order of 0,2 km^3 annually, this is not accounted for here.

3.3 The mass balance record for Vatnajökull.

From the digital mb maps (Fig. 4) the glacier wide volumes of winter, summer and net balances for Vatnajökull (and selected outlets) have been calculated by integration and are as follows:

B_w = 13,22 km^3_{we} ; b_w = 1,71 m_{we}
B_s = -21,96 km^3_{we} ; b_s = -2,84 m_{we}
B_n = -8,74 km^3_{we} ; b_n = -1,13 m_{we}
AAR = 49%

(balance values as a function of elevation are tabulated in appendix D) The weather in the autumn and first winter months 2018_19, was wet and rather warm, not much snowfall below ~1000 m. The latter half of the winter was also relatively warm with more than average precipitation, especially in the SE. The spring was warm and dry, and the thin winter snow of the highland melted quickly and winds blew dirt from there over the glacier and enhanced melt, especially in the accumulation zone. The total winter balance was ~6% higher than average (over the observation period from 1991_92, Fig. 14). The zero mass balance mass turnover for Vatnajökull (current topography) is close to 13,5 km^3_{we} (1,7 m_{we}) and the winter balance 2018_19 is ~2% lower (the zero mass

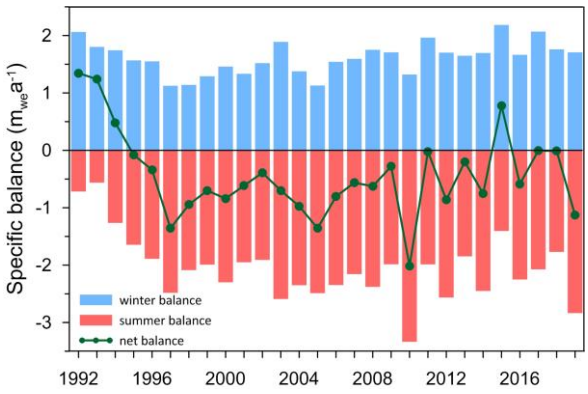

Figure 14. Specific mass balance record for Vatnajökull 1991 92 – 2018 19.

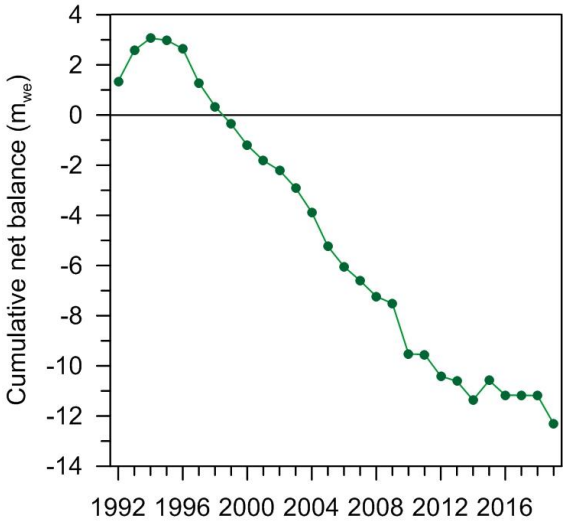

Figure 15. Cumulative specific mass balance of Vatnajökull 1991_92 – 2018_19.

turnover is estimated from the zero bn crossover when b_w, and b_s of the survey period are plotted against b_n).
The summer months were mostly warm and dry, but prevailing E and NE winds kept E-Iceland cold and cloudy for long periods. This explains the great difference in summer balance between the N and NE outlets and the S and SW outlets. The high summer mass loss in the accumulation area is due to unusually widely spread surface dirt for most of the summer. The total summer mass loss was ~30% more than the average since 1995 (almost 40% more since 1992). As mentioned above, zero mass balance turnover for Vatnajökull (current topography) is close to 13,5 km^3_{we} (1,7 m_{we}), the summer mass loss 2018 was 22 km^3_{we} or ~40 % more loss than the zero balance mass turnover. The summer mass loss this year was second only to that of the exceptional mass loss of 2009_10 (that was greatly affected by the tephra from the Eyjafjallajökull

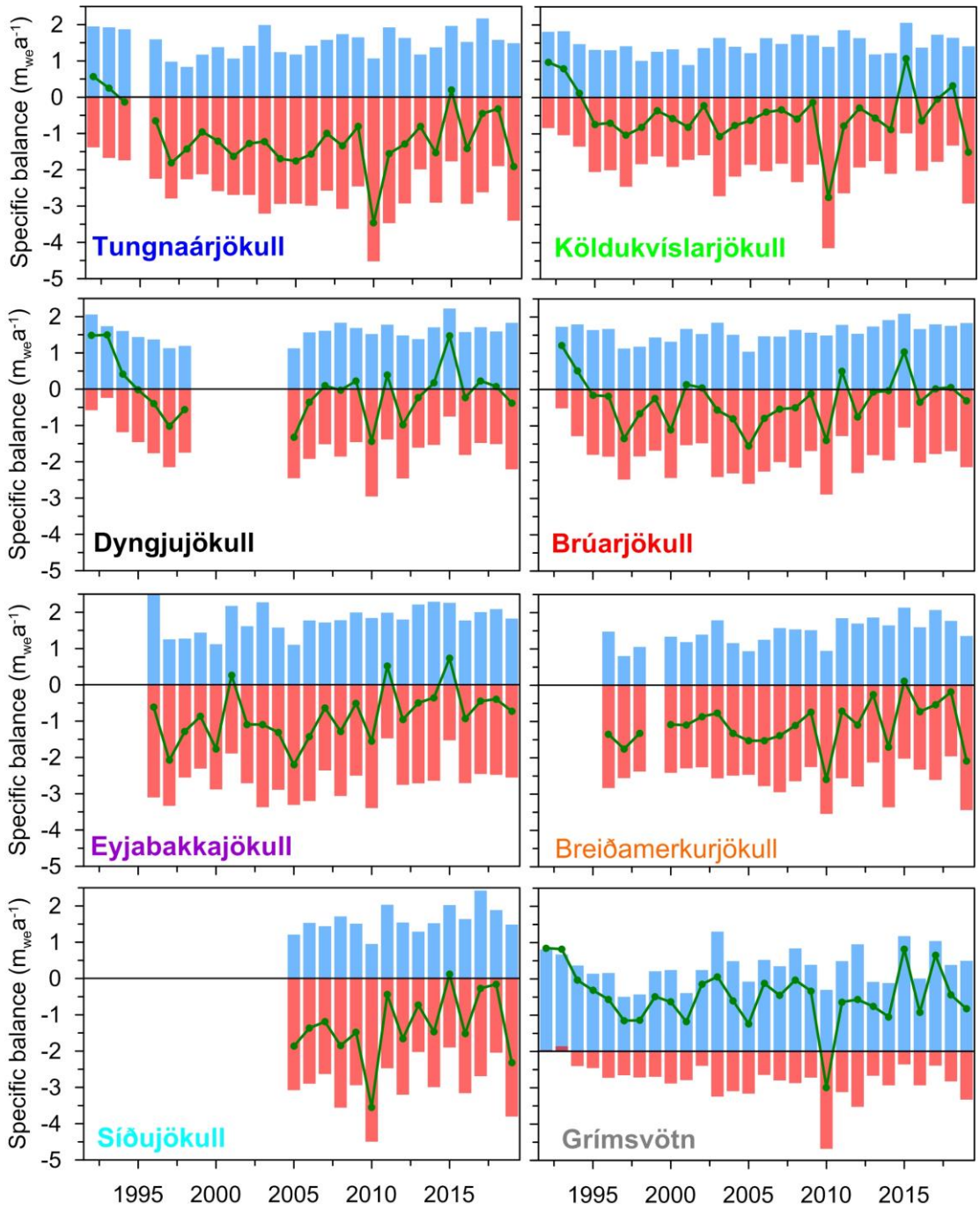

Figure 16. Specific mass balance record for Vatnajökull outlets 1991_92-2018_19.

eruption). The annual balance is among the four years with highest mass loss (the higher are 2009_10, 2004_5 and 1996_97) 90% more than average. The net balance has been negative since 1994_95 (except for 2014_15). After a short period of positive and close to zero mass balance, this year is comparable to the 20 year period of high mass loss.

The variability of the winter balance (Fig. 16) is by far more prominent for the outlets closest to sea. That part of the glacier receives precipitation from all south and east wind directions, and thus has high snow accumulation in winters when the paths of the North Atlantic low pressure systems are just south and east of Iceland.

During the period of high net mass loss since 1994_95, the northern outlets have had several years of close to zero and positive mass balance.

The cumulative net balance curves for the outlets of Vatnajökull in Fig. 17 show that all outlets have been losing mass since 1994_95. The slope for mass loss is about 0,7 $m_{we}a^{-1}$ for the northern outlets but 1,5 $m_{we}a^{-1}$ for the south and western outlets.

In Fig. 18 the relation of the annual net balance to the accumulation area ratio (AAR) and equilibrium line altitude (ELA) is shown for different outlets over the survey period. The b_n-AAR gradient is similar for all outlets, about 0,5 m_{we} for 10% change in AAR. The zero-balance AAR varies for different outlets in the range 60-65%, similar for all outlets except for the southern outlet Breiðamerkurjökull. Breiðamerkurjökull is far from equilibrium, the ablation area is too large. A large part of the outlet has carved 200-300 m deep through into the former sediment bed, and the surface and bed elevation has lowered accordingly. Similarly, the zero-balance ELA varies from about 1000-1100 m a.s.l. for the southern outlets to 1400 m a.s.l. for the NW outlets. The b_n-ELA slope is similar for all outlets -0,7 m_{we} per 100 m, except Eyjabakkajökull with a slope of -1,0 m_{we} per 100 m.

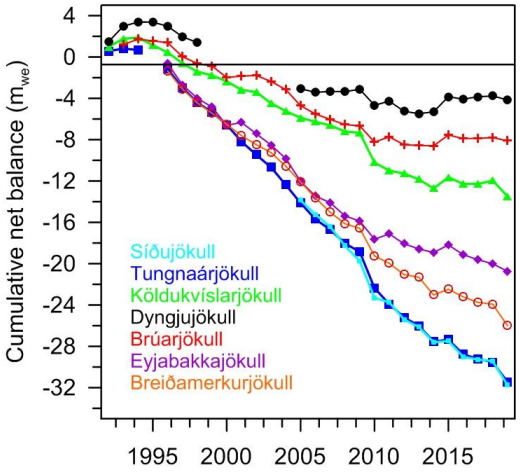

Figure 17. Cumulative specific surface mass balance for several of Vatnajökull outlets 1991_92 – 2018_19.

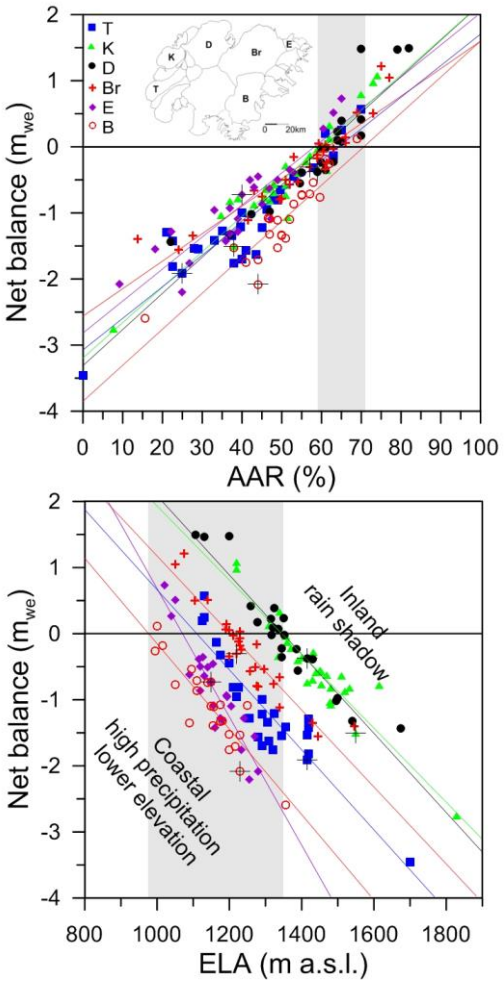

Figure 18. The relation between net annual balance (b_n) and accumulation area ratio (AAR) (upper) and b_n and equilibrium line altitude (ELA), for Vatnajökull outlets during the survey period. (This years points are marked with a black +).

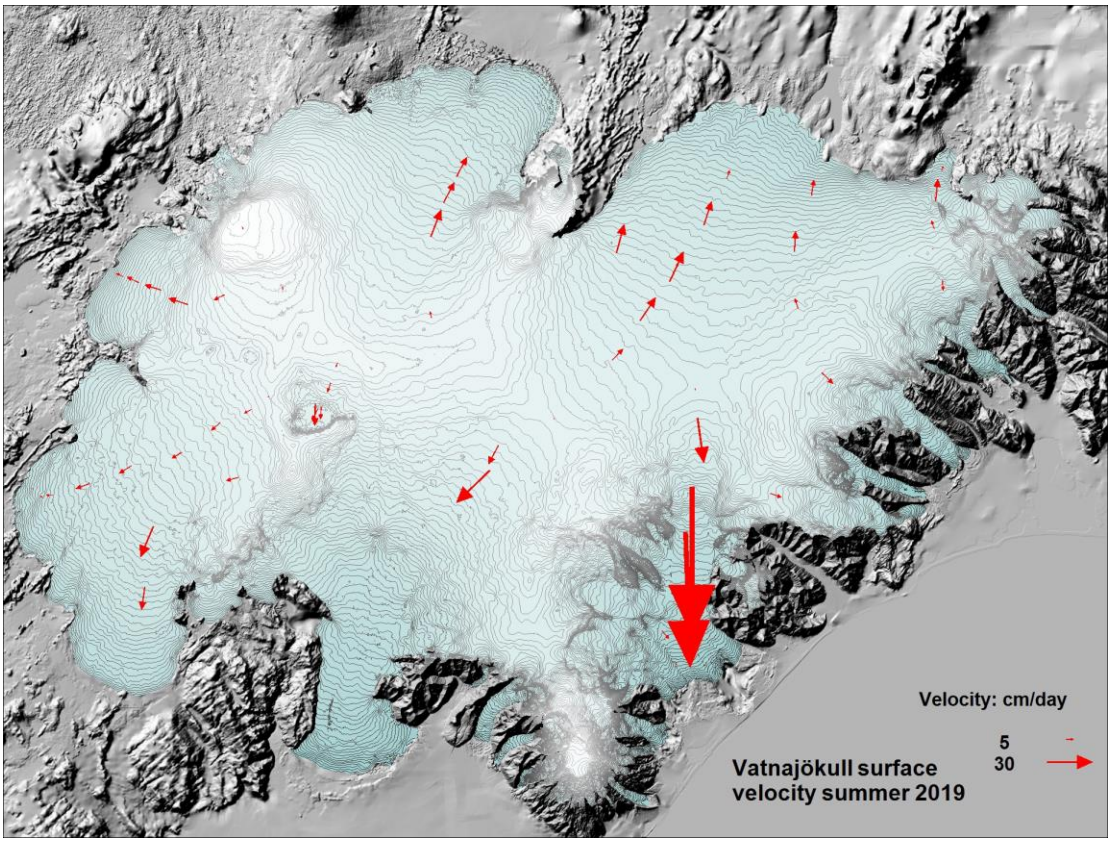

Figure 19. Average summer surface velocity at survey sites in 2018_19.

4. SURFACE VELOCITY MEASUREMENTS

The surface velocity of the glacier was calculated from DGPS (accuracy within 1 m), fast static (accuracy ~1 cm) and kinematic GPS (accuracy about ~10 cm) positioning of the ablation stakes. All sites were surveyed in spring and autumn (most kinematic, some DGPS), and many also in June (kinematic), August (fast static) and October (kinematic). At a few sites stakes from previous years were found and resurveyed, making it possible to calculate surface velocity over a year or longer time span. The average summer surface velocity is shown in Figure 19.

At sites close to the glacier terminus very small horizontal movement is measured. This indicates that the glacier snouts are almost stagnant. In the centre areas of some of the outlets especially close to the equilibrium line, there is an increase in velocity during summer compared to winter. The summer velocity is typically in the order of two-fold the winter velocity. This suggests that basal sliding is increased in the melting season, and is of the same magnitude as the deformation velocity.

To better understand the variable velocity continuous GPS has been run during summer at several sites.

From previous velocity measurements, surging of outlets has been predicted. Currently increase in velocity at sites D05 and D07 (Fig. 20.) suggests that Dyngjujökull may surge within a few years. The velocity at sites D07 and D05 is now similar to that in 1997 prior to the surge in 1998-2000 and the accumulation zone has thickened. To monitor velocity changes leading up to a surge 2 masts (going down with the melting surface) equipped with GPS

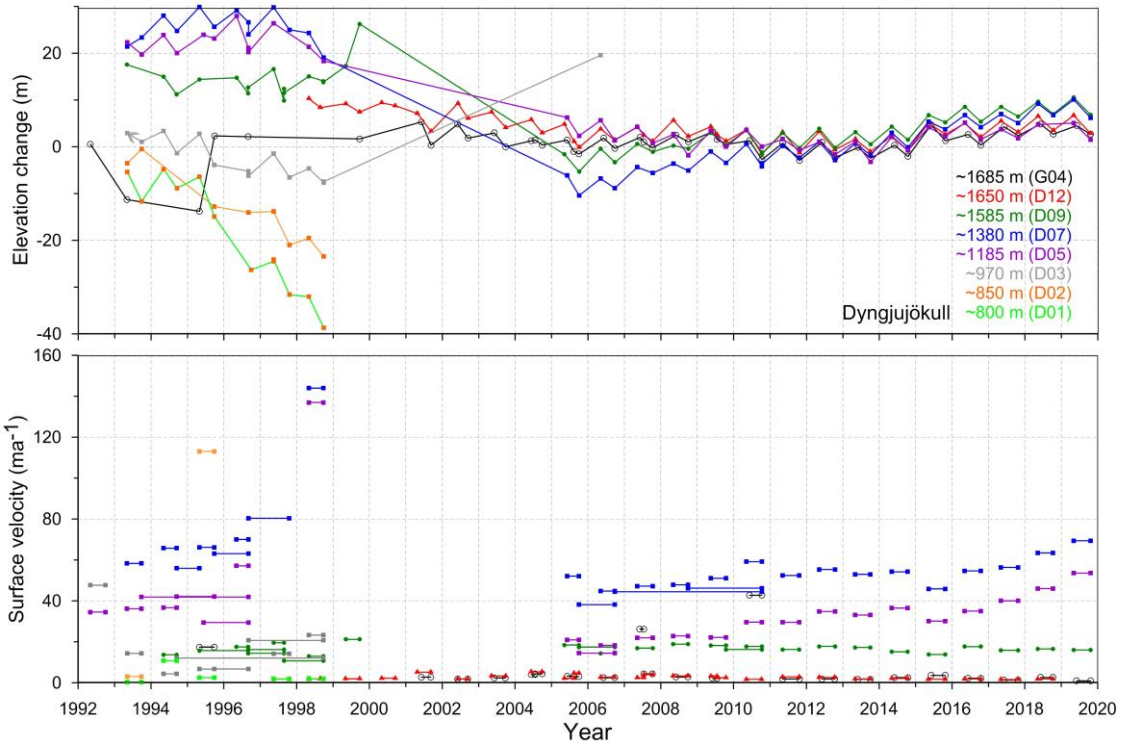

Figure 20. Surface elevation change relative to spring 2010 (upper panel) and average surface velocity (lower panel) at mb sites on Dyngjujökull in 1992 to 2019.

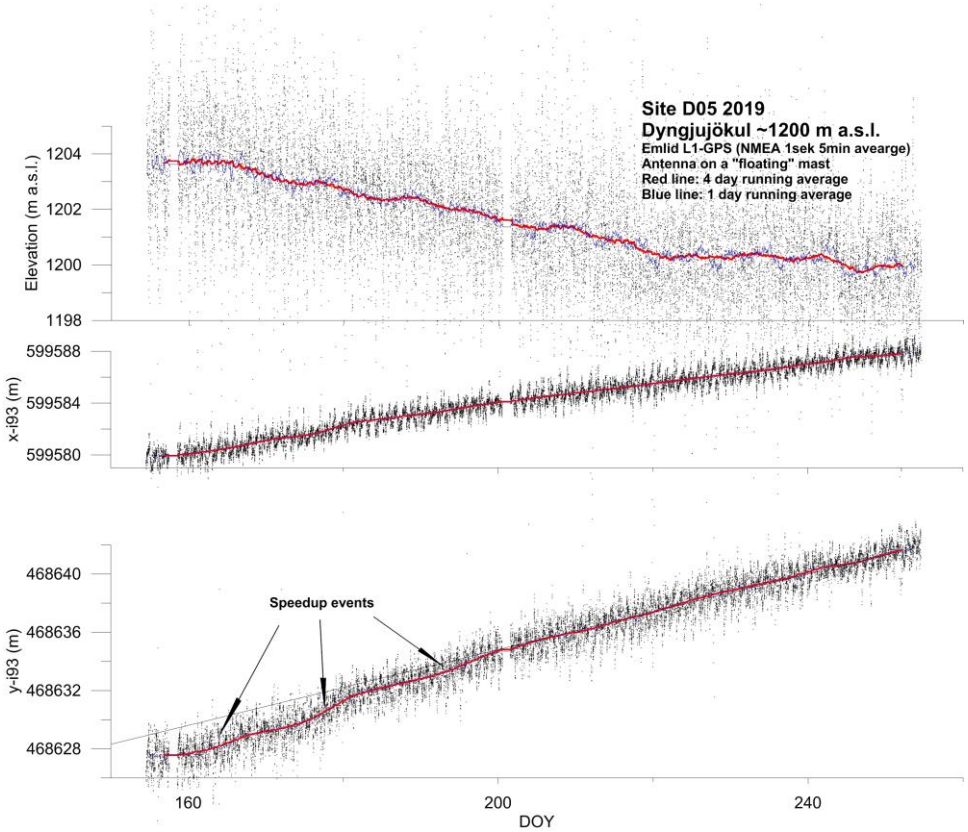

Figure 21 a. Surface elevation (top panel) and movement (easting in middle panel and northing in lowest panel) surveyed with continuous GPS survey at mb site D05 on Dyngjujökull in summer 2019.

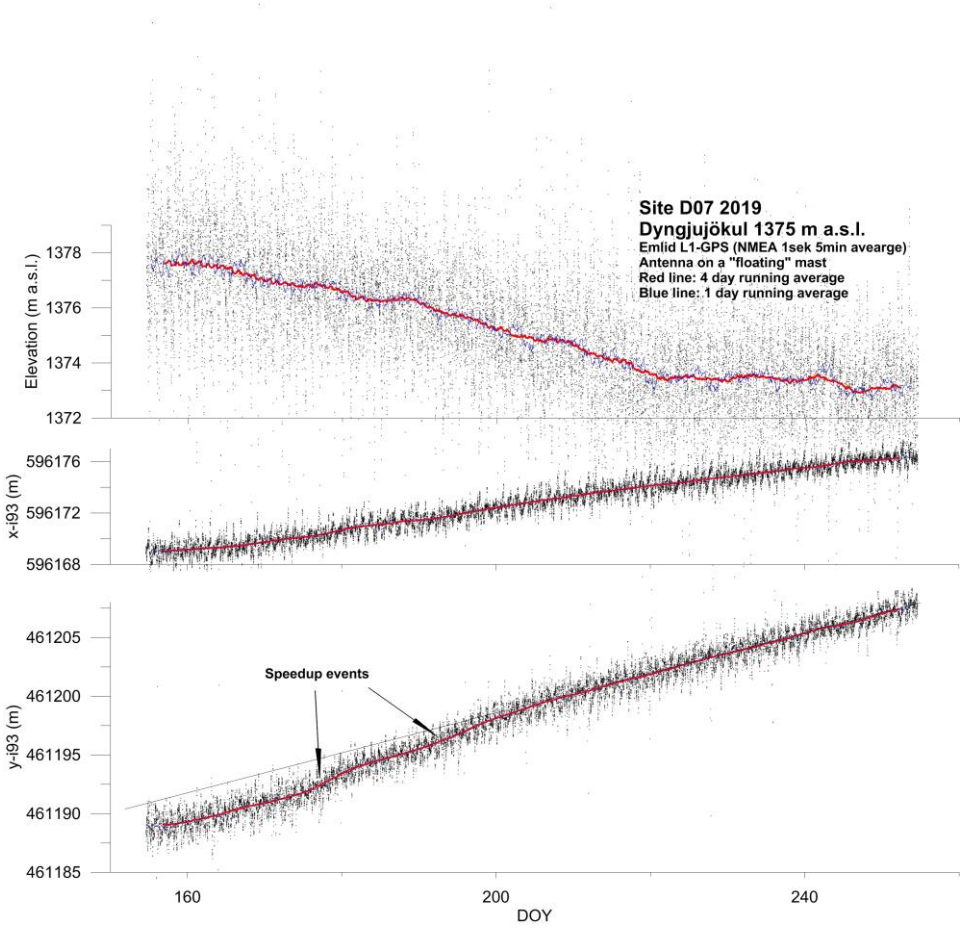

Figure 21 b. Surface elevation change (top panel) and movement (easting in middle panel and northing in lowest panel) surveyed with continuous GPS survey at mb site D07 on Dyngjujökull in summer 2019.

allows for monitored 3D motion at sites D05 and D07. The data collected allows for postprocessing to acquire more accuracy (~dm instead of ~m), but the processing has not been finished when this report is written. However the unprocessed data (Fig. 21a and 21b) show mostly steady movement except for 3 speedup events in June due to increase in meltwater and still undeveloped channel system at the glacier bed. The measured elevation shows that melting halts at day ~220 (mid-August) but there is a spell of melt for a few days in the first week of September.

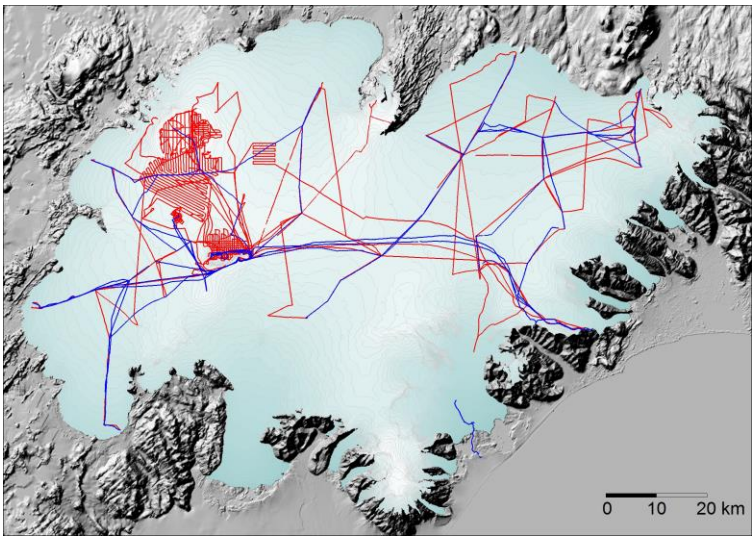

Figure 22. Location of surface elevation profiles surveyed in field trips on Vatnajökull in 2019. Survey in spring is shown with red and autumn survey in blue.

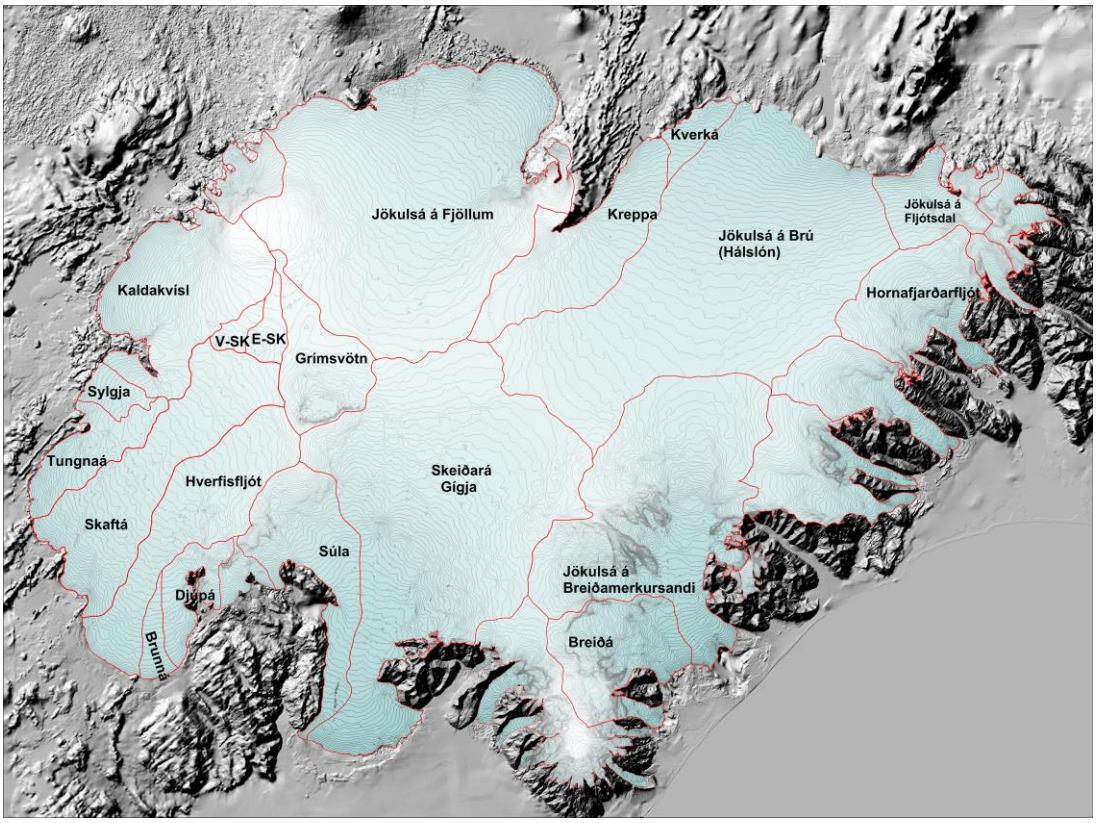

Figure 23. Water divides and drainage basins of selected rivers draining water from Vatnajökull.

5. Melt water runoff.

Water divides and drainage basins for rivers draining water from Vatnajökull have been defined from water pressure potential maps. The potential maps were produced from surface (year 2010) and bedrock DEMs.

Figure 23 shows the water divides and drainage areas for selected rivers draining melt water from Vatnajökull. The summer balance over the water basin is an estimate of meltwater contribution to rivers and groundwater storage. This estimate, however, does not include precipitation that falls as rain on the glacier, or snow that falls and melts during the summer. The meltwater contribution can be compared with river runoff at stream flow gauges closest to the glacier. For this comparison, we define the glaciological year from the start of October to the end of September and the period draining meltwater from the glacier during the summer from June through September. It would be misleading to include May in the summer period because runoff from the glacier melt in May is delayed due

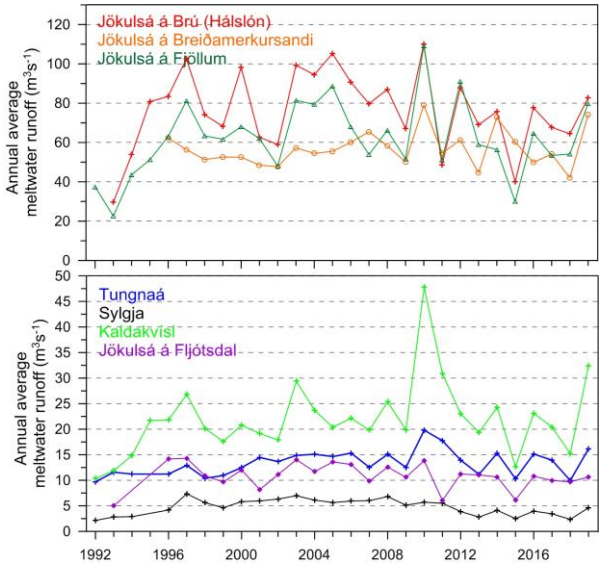

Figure 24. The temporal variation of average annual meltwater runoff to selected river catchments.

Table I. Melt water drainage to selected rivers.

Water Catchment:	Area (km^2)	ΣQ_s ($10^6 m^3$)	Q_s ($m^3 s^{-1}$)	Q_a ($m^3 s^{-1}$)	q_s ($ls^{-1} km^{-2}$)
Vatnajökull	7743,0	21958,9	2083,2	696,3	89,9
Tungnaá	119,0	510,1	48,4	16,2	135,9
Sylgja	39,5	146,0	13,9	4,6	117,2
Kaldakvísl	364,6	1022,4	97,0	32,4	88,9
Jökulsá á Fjöllum	1155,2	2521,9	239,3	80,0	69,2
Kreppa	290,8	528,8	50,2	16,8	57,7
Kverka	46,7	200,1	19,0	6,3	135,9
Jökulsá á Brú	1213,7	2608,7	247,5	82,7	68,2
Jökulsá á Fljótsdal	130,7	335,7	31,8	10,6	81,4
Jökulsá í Lóni	101,5	281,4	26,7	8,9	87,9
Hornafjarðarfljót	238,9	753,3	71,5	23,9	100,0
Jökulsá á Breiðamerkursandi	737,4	2339,9	222,0	74,2	100,6
Breiðá-Fjallsá	233,7	1126,5	106,9	35,7	152,9
Skeiðará-Gígja	1153,4	3393,8	322,0	107,6	93,3
Súla	252,8	1033,0	98,0	32,8	129,6
Brunná	34,9	197,8	18,8	6,3	179,7
Djúpá	79,0	366,7	34,8	11,6	147,2
Hverfisfljót	315,4	1031,5	97,9	32,7	103,7
Skaftá	389,7	1320,1	125,2	41,9	107,4
Grímsvötn	173,3	211,4	20,1	6,7	38,7
Eystri Skaftárketill	39,3	39,0	3,7	1,2	31,5
Vestari Skaftárketill	25,1	30,4	2,9	1,0	38,4
Hólmsá	164,8	556,0	52,7	17,6	107,0
Heinabergsvötn	229,5	856,2	81,2	27,1	118,3
Skjálfandafljót	96,8	163,9	15,5	5,2	53,7

ΣQ_s: total summer melt water; Q_s: average runoff (averaged over summer, 4 months, June – September)
Q_a: average runoff (averaged over a whole year); q_s : average runoff per km^2 (averaged over a whole year)

to refreezing during elimination of the cold wave and because of the contribution of the spring snow melt from the highlands to the runoff. Some melting also occurs during winter, especially in the terminus regions of the southern outlets.

Average melt water runoff to different rivers is given in Table I, and temporal variation of the average meltwater runoff in Fig. 24. The average specific runoff (q_s) differs from basin to basin from ~10 to ~140 $ls^{-1}km^{-2}$. This is mainly due to different elevation distributions, for example, the water drainage basins for Tungnaá and Kverká are within the ablation area, while that of Grímsvötn and Skaftárkatlar are high in the accumulation zone.

6. Conclusions

In the glaciological year 2018_19 the winter balance for Vatnajökull exceeded the average, over the observation period from 1991_92, by ~6%.
The total summer mass loss was 30% more than average since 1995 (~40% more than average since 191_92).
The net balance was negative as it has been since 1994_95 (except 2014_15), almost twofold the average since 1994_95 (2,7-times the average since 1991_92).
In the past few years, the about 20 year period of high mass loss seemed to have halted; but this year the mass loss is high again.
The total mass loss over the 27 year survey period is 12,1 m_{we} (ice volume of ~109 km^3) since 1991_92 (or since 1994_95, 15,5 m_{we}, ice volume of ~136 km^3)). The volume loss since 1991_92 amounts to ~3,6% of total ice volume (~4,5% since 1994_95).
In addition to surface melt, mass is lost due to calving, geothermal melting at the glacier bed and melt from frictional energy due to ice deformation and sliding. This is estimated to be close to 0,2 $m_{we}a^{-1}$ for Vatnajökull (Jóhannesson Tómas, Bolli Pálmason, Árni Hjartarson, Alexander H. Jarosch, Eyjólfur Magnússon, Joaquín M. C. Belart og Magnús Tumi Guðmundsson. *Non-surface mass balance of glaciers in Iceland*. Submitted to *Journal of Glaciology* in Dec 2019).
Glacier surface meltwater runoff in summer 2019 (estimated from summer surface balance only, summer rain and snow that falls and melts during summer, calving and geothermal melting, is not included; averages refer to the survey period of each outlet): to Tungnaá 20% more than average, 48 % more than average to Kaldakvísl, 27% more than average to Jökulsá á Fjöllum, 8% more than average to Hálslón, close to average to Jökulsá í Fljótsdal and 30% more than average to Jökulsá á Breiðamerkursandi.
Surface velocity measurements suggest that Dyngjujökull is in the first phase of a surge, and will likely complete a surge cycle within the next few years.

Mass balance summary 2018_19:

B_w = 13,22 km^3_{we}
B_s = -21,96 km^3_{we}
B_n = -8,74 km^3_{we}
AAR = 49%

Specific Values:

b_w = 1,71 m_{we}
b_s = -2,84 m_{we}
b_n = -1,13 m_{we}

Appendix A: Surface mass balance at measurement sites 2018_19.

b_w: specific winter balance, **b_s**: specific summer balance, **b_n**: specific net balance, **l_a**: new snow in autumn (all in water equivalent).

Site	Position				Elevation	Date	Date	b_w	b_s	b_n	la
	Latitude		Longitude		(m a.s.l.)	in spring	in autumn	(m)	(m)	(m)	(m)
B09-19	64	44,8437	16	5,8577	724,9	20190503	20191019	0,00	-5,760	-5,760	0,01
B10-19	64	43,6873	16	6,6986	779,3	20190503	20191019	0,06	-4,857	-4,802	0
B11-19	64	40,9687	16	10,4534	950,0	20190503	20191019	0,64	-3,457	-2,819	0,03
B12-19	64	38,2613	16	14,1359	1077,5	20190503	20191019	1,08	-2,457	-1,377	0,1
B13ror15	64	34,5882	16	19,6556	1218,2	20190503	20191019	1,78	-1,819	-0,041	0,15
B14-19	64	31,6436	16	24,7042	1322,4	20190503	20191019	2,01	-1,751	0,264	0,26
B15-19	64	28,4918	16	30,0250	1405,8	20190503	20191019	2,30	-1,504	0,792	0,32
B16-19	64	24,1291	16	40,8777	1528,4	20190530	20191019	2,32	-1,165	1,152	0,35
B17-19	64	36,7343	16	28,7938	1216,9	20190501	20191019	1,54	-2,116	-0,576	0,21
Br1-19	64	5,8367	16	19,7107	104,1	20190501	20191127	-2,85	-10,750	-13,600	0
Br2-19	64	6,3640	16	22,5339	192,1	20190501	20191127	-2,65	-7,970	-10,620	0
Br3-19	64	8,4539	16	24,0241	375,6	20190501	20191128	-2,35	-7,300	-9,650	0
Br5-19	64	13,5372	16	19,2007	676,6	20190501	20190000	0,00			
Br7-18	64	22,1651	16	16,9270	1248,8	20190501	20191018	2,12	-1,942	0,180	0,23
B07-19	64	25,8005	16	17,4642	1359,7	20190501	20191018	2,55	-1,375	1,170	0,2
BB0-19	64	22,7107	16	5,0524	1521,8	20190501	20191018	3,73	-1,285	2,448	0,49
Bru-19	64	39,7482	15	56,5404	896,7	20190502	20191019	0,78	-3,615	-2,838	0,04
Bud-19	64	35,9894	15	59,8926	1138,2	20190502	20191018	1,43	-2,339	-0,910	0,22
B18-19	64	31,5771	16	0,1398	1316,2	20190501	20191018	2,43	-1,318	1,116	0,24
B19-19	64	27,9977	15	55,9859	1441,4	20190501	20191018	3,71	-1,167	2,544	0,63
BB0-19	64	22,7107	16	5,0524	1521,8	20190501	20191018	3,73	-1,285	2,448	0,49
D05-19	64	42,2250	16	54,6968	1205,2	20190504	20191020	1,34	-3,162	-1,827	0,09
D07-19	64	38,2821	16	59,2624	1378,7	20190504	20191020	1,85	-2,060	-0,206	0,14
D09-19	64	31,7983	17	0,5971	1587,6	20190504	20191020	2,26	-1,250	1,014	0,14
D12-19	64	28,9736	17	0,1772	1651,2	20190504	20191020	2,20	-1,047	1,152	0,26
E01-19	64	40,6289	15	34,8637	766,2	20190502	20191019	0,06	-5,289	-5,234	0
E02-19	64	39,1251	15	35,9853	952,3	20190502	20191019	1,03	-3,316	-2,288	0,04
E03-19	64	36,6616	15	36,9252	1190,0	20190502	20191019	2,07	-1,586	0,480	0,15
E04-19	64	34,9514	15	37,1484	1291,2	20190501	20191019	2,82	-1,707	1,116	0,25
K01-19	64	35,1694	17	51,8322	1049,1	20190505	20191020	0,30	-6,096	-5,795	0
K02-19	64	34,8068	17	49,6700	1173,3	20190505	20191020	0,54	-5,400	-4,856	0,01
K03-19	64	34,2372	17	46,3922	1296,4	20190505	20191020	0,96	-3,516	-2,555	0,02
K04-19	64	33,2111	17	42,2485	1489,3	20190505	20191020	1,68	-2,040	-0,361	0,04
K05-19	64	33,4462	17	35,4531	1681,6	20190505	20191020	2,06	-1,259	0,804	0,23
K06-19	64	38,3494	17	31,3488	1946,1	20190601	20191020	2,78	-0,594	2,184	0,44
K07-19	64	29,1068	17	42,0416	1534	20190505	20191020	1,96	-1,448	0,516	0,04
S01-19	64	7,0017	17	49,9683	719,4	20190505	20191129	0,00	-6,129	-6,129	0
S02-19	64	12,1551	17	48,9784	1005	20190505	20191021	1,17	-4,905	-3,735	0
S04-19	64	16,1735	17	48,2027	1160	20190505	20191021	1,63	-3,835	-2,208	0,09
S05-19	64	20,5005	17	33,9973	1454	20190504	20191021	2,61	-1,971	0,642	0,11
Haab-19	64	20,9598	17	24,1173	1732,2	20190606	20191020	3,60	-1,227	2,374	0,19

T01-19	64	20,0662	18	6,8416	778,8	20190506	20191129	0,00	-7,875	-7,875	0
T01ve-19	64	19,4705	18	5,2657	876,3	20190506	20191021	0,00	-5,445	-5,445	0
T02-19	64	19,6010	18	3,9968	924,6	20190505	20191021	0,57	-4,845	-4,271	0
T03-19	64	20,2031	17	58,5838	1071,0	20190505	20191021	1,33	-3,895	-2,562	0
T04-19	64	21,3326	17	51,5154	1222,9	20190505	20191021	1,65	-3,297	-1,649	0,09
T05-19	64	22,2682	17	42,9937	1347,7	20190505	20191021	1,90	-2,740	-0,836	0,15
T06-19	64	24,2675	17	36,5079	1470,7	20190505	20191021	2,28	-1,522	0,762	0,15
T07-18	64	25,2959	17	31,1973	1566,2	20190504	20191020	2,32	-1,674	0,642	0,1
T08-19	64	26,2920	17	27,7549	1639,2	20190504	20191020	2,43	-1,180	1,248	0,18
Borth-17	64	25,0441	17	19,1796	1406,0	20190504	20191022	2,41	-2,210	0,198	0,22
Bor-19	64	24,9400	17	20,1388	1405,1	20190606	20191022	2,62	-2,347	0,276	0,22
G02-19	64	26,8444	17	17,7163	1566,0	20190602	20191020	2,00	-0,972	1,032	0,08
G03-19	64	28,4354	17	16,3319	1660,0	20190602	20191020	2,46	-1,021	1,434	0,23
G04-19	64	30,0169	17	15,0478	1689,0	20190602	20191020	2,59	-0,849	1,740	0,14
Go1-19	64	33,9742	17	24,9551	1760,6	20190601	20191020	2,32	-0,865	1,452	0,19
Skf00-19	64	15,4626	15	54,0717	953,0	20190430	20191022	1,94	-3,722	-1,779	0
Hof01-19	64	32,3358	15	35,8447	1144,5	20190501	20191019	2,94	-2,408	0,528	0,12
Skf01-18	64	18,0078	16	4,9859	1285,9	20190430	20191018	3,66	-1,888	1,776	0,35
Fl01-19	64	26,1555	15	55,6236	1349,7	20190501	20191018	3,75	-1,37	2,3823	0,4
Barc-19	64	38,4090	17	26,7797	1894,9	20190601		2,49			
Ske02-19	64	18,1605	17	9,1837	1209,0	20190504		1,54			
Ske03-19	64	17,7995	17	0,0029	1254,1	20190504		1,55			
Ske04-19	64	19,4978	16	54,5151	1368,3	20190504	20191019	2,11	-1,983	0,132	0,21
Ske05-19	64	21,6992	16	51,0299	1436	20190504	20191019	2,49	-1,797	0,696	0,26

Appendix B: Surface mass balance distribution by elevation in 2018_19.

ΔS : area in elevation range, ∑ΔS: cumulative area above given elevation, b_w: specific winter balance, b_s: specific summer balance. b_n: specific winter balance, ΔB_w : winter balance at a given elevation range, $\sum\Delta B_w$: cumulative winter balance above given elevation, ΔB_s summer balance at a given elevation range, $\sum\Delta B_s$: cumulative summer balance above given elevation, ΔB_n: net annual balance in a given elevation range, $\sum B_n$: cumulative net annual balance above given elevation.

Vatnajökull

Elevation (m a.s.l.)			ΔS (km^2)	∑ΔS (km^2)	b_w (mm)	b_s (mm)	b_n (mm)	ΔB_w ($10^6 m^3$)	$\sum\Delta B_w$ ($10^6 m^3$)	ΔB_s ($10^6 m^3$)	$\sum\Delta B_s$ ($10^6 m^3$)	ΔB_n ($10^6 m^3$)	$\sum B_n$ ($10^6 m^3$)
2000	2050	2025	0,4	0,4	6142	-333	5808	2,8	2,8	-0,1	-0,1	2,6	2,6
1950	2000	1975	8,8	9,2	3292	-601	2690	28,8	31,6	-5,3	-5,4	23,6	26,2
1900	1950	1925	36,6	45,8	2824	-619	2205	103,3	134,9	-22,6	-28,1	80,6	106,8
1850	1900	1875	47,4	93,2	2985	-682	2303	141,5	276,4	-32,3	-60,4	109,1	216,0
1800	1850	1825	46,9	140,1	3288	-676	2612	154,4	430,7	-31,7	-92,1	122,6	338,6
1750	1800	1775	54,3	194,4	2894	-791	2103	157,3	588,0	-43,0	-135,1	114,3	452,9
1700	1750	1725	104,0	298,4	2600	-909	1691	270,6	858,6	-94,6	-229,7	176,0	628,9
1650	1700	1675	221,6	520,0	2547	-1006	1540	564,5	1423,1	-223,1	-452,8	341,4	970,3
1600	1650	1625	372,5	892,5	2494	-1116	1378	929,3	2352,5	-415,9	-868,7	513,4	1483,7
1550	1600	1575	353,0	1245,5	2459	-1236	1223	868,4	3220,8	-436,4	-1305,1	432,0	1915,7
1500	1550	1525	419,5	1665,0	2419	-1350	1068	1014,9	4235,7	-566,6	-1871,7	448,3	2364,1
1450	1500	1475	452,0	2117,0	2450	-1516	934	1107,6	5343,3	-685,4	-2557,0	422,2	2786,3
1400	1450	1425	502,0	2619,0	2528	-1655	872	1269,2	6612,5	-831,2	-3388,2	438,0	3224,3
1350	1400	1375	545,8	3164,8	2464	-1797	667	1345,3	7957,9	-981,1	-4369,3	364,3	3588,6
1300	1350	1325	536,3	3701,1	2303	-2026	277	1235,6	9193,5	-1086,8	-5456,1	148,8	3737,4
1250	1300	1275	506,2	4207,3	2165	-2245	-80	1096,0	10289,5	-1136,6	-6592,7	-40,6	3696,8
1200	1250	1225	444,3	4651,6	1954	-2549	-595	868,3	11157,8	-1132,6	-7725,3	-264,3	3432,5
1150	1200	1175	395,7	5047,3	1744	-2849	-1104	690,2	11847,9	-1127,4	-8852,7	-437,2	2995,3
1100	1150	1125	356,7	5404,0	1581	-3122	-1540	564,1	12412,0	-1113,8	-9966,4	-549,7	2445,6
1050	1100	1075	313,7	5717,7	1404	-3394	-1989	440,7	12852,7	-1064,8	-11031,2	-624,1	1821,4
1000	1050	1025	294,3	6012,0	1209	-3724	-2515	356,0	13208,6	-1096,1	-12127,3	-740,1	1081,3
950	1000	975	263,6	6275,6	1011	-4037	-3025	266,7	13475,3	-1064,4	-13191,6	-797,6	283,7
900	950	925	228,5	6504,1	834	-4343	-3509	190,7	13666,0	-992,7	-14184,4	-802,1	-518,4
850	900	875	204,1	6708,2	643	-4684	-4040	131,5	13797,5	-956,3	-15140,6	-824,8	-1343,2
800	850	825	182,4	6890,6	459	-5096	-4637	83,8	13881,3	-929,8	-16070,5	-846,0	-2189,2
750	800	775	156,2	7046,8	273	-5523	-5249	42,7	13924,0	-862,7	-16933,2	-820,0	-3009,2
700	750	725	124,1	7170,9	120	-5915	-5794	15,0	13938,9	-734,0	-17667,2	-719,1	-3728,3
650	700	675	95,2	7266,1	12	-6060	-6048	1,2	13940,1	-577,0	-18244,3	-575,9	-4304,2
600	650	625	59,9	7326,0	-213	-6229	-6442	-12,8	13927,3	-373,3	-18617,6	-386,1	-4690,2
550	600	575	63,2	7389,2	-592	-6517	-7109	-37,4	13889,9	-411,7	-19029,3	-449,1	-5139,3
500	550	525	46,4	7435,6	-818	-6732	-7551	-38,0	13851,9	-312,3	-19341,6	-350,3	-5489,7
450	500	475	39,0	7474,6	-1168	-6933	-8101	-45,6	13806,3	-270,7	-19612,3	-316,4	-5806,0
400	450	425	43,8	7518,4	-1503	-7162	-8666	-65,9	13740,4	-313,7	-19926,0	-379,6	-6185,6
350	400	375	39,0	7557,4	-1823	-7517	-9340	-71,1	13669,3	-293,3	-20219,4	-364,5	-6550,1
300	350	325	37,0	7594,4	-2032	-8010	-10042	-75,2	13594,1	-296,4	-20515,7	-371,6	-6921,7
250	300	275	35,6	7630,0	-2202	-8355	-10558	-78,5	13515,6	-297,7	-20813,5	-376,2	-7297,9
200	250	225	36,0	7666,0	-2357	-8881	-11238	-85,0	13430,6	-320,1	-21133,5	-405,0	-7702,9
150	200	175	31,1	7697,1	-2541	-9989	-12530	-79,0	13351,7	-310,5	-21444,0	-389,5	-8092,4
100	150	125	24,6	7721,7	-2709	-10834	-13543	-66,6	13285,1	-266,2	-21710,2	-332,8	-8425,1
50	100	75	13,4	7735,1	-2826	-11368	-14194	-37,8	13247,2	-152,2	-21862,4	-190,1	-8615,2
0	50	25	8,1	7743,2	-2887	-11876	-14764	-23,4	13223,8	-96,4	-21958,9	-119,9	-8735,1

Tungnaárjökull

Elevation (m a.s.l.)			ΔS (km^2)	∑ΔS (km^2)	b_w (mm)	b_s (mm)	b_n (mm)	ΔB_w ($10^6 m^3$)	$\sum\Delta B_w$ ($10^6 m^3$)	ΔB_s ($10^6 m^3$)	$\sum\Delta B_s$ ($10^6 m^3$)	ΔB_n ($10^6 m^3$)	$\sum B_n$ ($10^6 m^3$)
1650	1700	1675	1,8	1,8	2350	-1103	1246	4,3	4,3	-2,0	-2,0	2,3	2,3
1600	1650	1625	12,7	14,5	2343	-1190	1152	29,9	34,2	-15,2	-17,2	14,7	17,0
1550	1600	1575	15,7	30,2	2270	-1302	968	35,6	69,8	-20,4	-37,7	15,2	32,2
1500	1550	1525	15,5	45,7	2235	-1368	867	34,7	104,5	-21,2	-58,9	13,5	45,6
1450	1500	1475	18,4	64,1	2202	-1496	706	40,4	145,0	-27,5	-86,4	13,0	58,6
1400	1450	1425	23,0	87,1	2157	-1968	189	49,5	194,5	-45,2	-131,5	4,3	63,0
1350	1400	1375	21,4	108,5	2018	-2482	-463	43,1	237,6	-53,0	-184,5	-9,9	53,1
1300	1350	1325	27,5	136,0	1856	-2887	-1030	51,1	288,7	-79,4	-264,0	-28,4	24,7
1250	1300	1275	21,1	157,1	1763	-3130	-1366	37,2	325,9	-66,1	-330,1	-28,9	-4,2
1200	1250	1225	23,1	180,2	1678	-3351	-1672	38,7	364,7	-77,4	-407,4	-38,6	-42,8
1150	1200	1175	21,0	201,2	1573	-3620	-2047	33,0	397,7	-76,0	-483,5	-43,0	-85,8
1100	1150	1125	18,4	219,6	1409	-3824	-2415	25,9	423,6	-70,3	-553,8	-44,4	-130,2
1050	1100	1075	19,1	238,7	1218	-3967	-2748	23,3	446,9	-75,9	-629,7	-52,6	-182,8
1000	1050	1025	17,4	256,1	989	-4235	-3246	17,3	464,2	-73,9	-703,6	-56,6	-239,4
950	1000	975	17,3	273,4	753	-4633	-3880	13,0	477,2	-80,0	-783,6	-67,0	-306,4
900	950	925	16,4	289,8	550	-5092	-4541	9,0	486,2	-83,3	-866,9	-74,3	-380,7
850	900	875	13,4	303,2	371	-5584	-5212	5,0	491,2	-74,8	-941,6	-69,8	-450,5
800	850	825	13,7	316,9	208	-6143	-5934	2,9	494,0	-84,0	-1025,6	-81,1	-531,6
750	800	775	9,6	326,5	38	-6743	-6705	0,4	494,4	-64,5	-1090,1	-64,1	-595,7
700	750	725	5,0	331,5	-94	-7221	-7315	-0,5	493,9	-36,2	-1126,3	-36,7	-632,3
650	700	675	0,4	331,9	-159	-7387	-7547	0,0	493,9	-3,0	-1129,2	-3,0	-635,4

Sylgjujökull

Elevation (m a.s.l.)			ΔS (km^2)	∑ΔS (km^2)	b_w (mm)	b_s (mm)	b_n (mm)	ΔB_w ($10^6 m^3$)	$\sum\Delta B_w$ ($10^6 m^3$)	ΔB_s ($10^6 m^3$)	$\sum\Delta B_s$ ($10^6 m^3$)	ΔB_n ($10^6 m^3$)	$\sum B_n$ ($10^6 m^3$)
1600	1650	1625	1,7	1,7	2156	-1235	920	3,7	3,7	-2,1	-2,1	1,6	1,6
1550	1600	1575	5,5	7,2	2103	-1301	802	11,5	15,2	-7,1	-9,2	4,4	6,0
1500	1550	1525	18,6	25,8	2028	-1412	615	37,7	52,8	-26,2	-35,5	11,4	17,4
1450	1500	1475	13,2	39,0	2023	-1560	463	26,7	79,5	-20,6	-56,0	6,1	23,5
1400	1450	1425	8,3	47,3	2019	-1953	65	16,7	96,2	-16,2	-72,2	0,5	24,0
1350	1400	1375	5,6	52,9	1974	-2469	-494	11,0	107,2	-13,8	-86,0	-2,8	21,3
1300	1350	1325	5,1	58,0	1867	-2969	-1101	9,6	116,8	-15,3	-101,2	-5,7	15,6
1250	1300	1275	10,1	68,1	1773	-3193	-1419	17,8	134,6	-32,1	-133,3	-14,3	1,3
1200	1250	1225	12,0	80,1	1687	-3303	-1616	20,3	154,9	-39,6	-173,0	-19,4	-18,1
1150	1200	1175	13,6	93,7	1562	-3465	-1902	21,3	176,2	-47,1	-220,1	-25,9	-43,9
1100	1150	1125	12,7	106,4	1336	-3688	-2352	17,0	193,2	-47,0	-267,1	-30,0	-73,9
1050	1100	1075	12,3	118,7	1114	-3894	-2780	13,7	206,8	-47,7	-314,8	-34,1	-108,0
1000	1050	1025	10,4	129,1	896	-4287	-3390	9,3	216,2	-44,6	-359,4	-35,3	-143,3
950	1000	975	3,0	132,1	701	-4571	-3870	2,1	218,3	-13,9	-373,3	-11,8	-155,0
900	950	925	1,1	133,2	597	-4806	-4208	0,7	218,9	-5,2	-378,6	-4,6	-159,6

Köldukvíslarjökul

Elevation (m a.s.l.)			ΔS (km^2)	∑ΔS (km^2)	b_w (mm)	b_s (mm)	b_n (mm)	ΔB_w ($10^6 m^3$)	$\sum\Delta B_w$ ($10^6 m^3$)	ΔB_s ($10^6 m^3$)	$\sum\Delta B_s$ ($10^6 m^3$)	ΔB_n ($10^6 m^3$)	$\sum B_n$ ($10^6 m^3$)
1950	2000	1975	0,8	0,8	2664	-584	2080	2,2	2,2	-0,5	-0,5	1,7	1,7
1900	1950	1925	13,9	14,7	2541	-606	1935	35,4	37,6	-8,4	-8,9	27,0	28,7
1850	1900	1875	6,4	21,1	2414	-716	1698	15,4	53,0	-4,6	-13,5	10,9	39,5
1800	1850	1825	6,0	27,1	2345	-808	1537	14,1	67,2	-4,9	-18,4	9,3	48,8
1750	1800	1775	10,3	37,4	2327	-829	1498	24,0	91,2	-8,6	-26,9	15,5	64,3
1700	1750	1725	17,0	54,4	2196	-994	1201	37,3	128,5	-16,9	-43,8	20,4	84,7
1650	1700	1675	15,9	70,3	2047	-1260	787	32,6	161,1	-20,0	-63,9	12,5	97,2
1600	1650	1625	14,1	84,4	1945	-1454	490	27,5	188,5	-20,6	-84,4	6,9	104,1
1550	1600	1575	18,7	103,1	1866	-1640	226	34,8	223,4	-30,6	-115,0	4,2	108,3
1500	1550	1525	20,3	123,4	1823	-1848	-25	37,0	260,4	-37,5	-152,6	-0,5	107,8
1450	1500	1475	19,4	142,8	1701	-2145	-443	33,0	293,4	-41,6	-194,2	-8,6	99,2
1400	1450	1425	15,2	158,0	1546	-2401	-854	23,5	316,9	-36,5	-230,7	-13,0	86,2
1350	1400	1375	15,1	173,1	1340	-2739	-1398	20,2	337,1	-41,2	-271,9	-21,1	65,2
1300	1350	1325	16,5	189,6	1129	-3236	-2106	18,6	355,8	-53,4	-325,3	-34,8	30,4
1250	1300	1275	17,7	207,3	899	-3853	-2953	15,9	371,6	-68,0	-393,4	-52,2	-21,7
1200	1250	1225	17,2	224,5	698	-4525	-3827	12,0	383,7	-77,9	-471,3	-65,9	-87,6
1150	1200	1175	16,2	240,7	541	-5107	-4566	8,8	392,4	-82,7	-554,0	-73,9	-161,5
1100	1150	1125	14,6	255,3	426	-5534	-5108	6,2	398,6	-80,6	-634,6	-74,4	-236,0
1050	1100	1075	12,8	268,1	341	-5911	-5569	4,4	403,0	-75,4	-710,0	-71,1	-307,0
1000	1050	1025	10,1	278,2	278	-6260	-5982	2,8	405,8	-63,5	-773,5	-60,7	-367,7
950	1000	975	8,1	286,3	229	-6549	-6319	1,9	407,7	-53,2	-826,7	-51,3	-419,0
900	950	925	2,5	288,8	185	-6737	-6551	0,5	408,1	-16,6	-843,3	-16,2	-435,2

Dyngjujökull

Elevation (m a.s.l.)			ΔS (km^2)	∑ΔS (km^2)	b_w (mm)	b_s (mm)	b_n (mm)	ΔB_w ($10^6 m^3$)	$\sum\Delta B_w$ ($10^6 m^3$)	ΔB_s ($10^6 m^3$)	$\sum\Delta B_s$ ($10^6 m^3$)	ΔB_n ($10^6 m^3$)	$\sum B_n$ ($10^6 m^3$)
2000	2050	2025	0,0	0,0	2494	-708	1785	0,0	0,0	0,0	0,0	0,0	0,0
1950	2000	1975	3,3	3,3	2570	-659	1910	8,4	8,5	-2,2	-2,2	6,3	6,3
1900	1950	1925	12,7	16,0	2555	-612	1942	32,5	40,9	-7,8	-10,0	24,7	31,0
1850	1900	1875	25,1	41,1	2481	-723	1758	62,4	103,3	-18,2	-28,1	44,2	75,2
1800	1850	1825	14,8	55,9	2462	-826	1635	36,4	139,7	-12,2	-40,3	24,2	99,3
1750	1800	1775	15,7	71,6	2445	-890	1554	38,3	178,0	-14,0	-54,3	24,4	123,7
1700	1750	1725	28,1	99,7	2459	-919	1540	69,1	247,1	-25,8	-80,1	43,3	167,0
1650	1700	1675	73,5	173,2	2474	-934	1539	181,7	428,9	-68,6	-148,8	113,1	280,1
1600	1650	1625	118,8	292,0	2377	-1072	1305	282,4	711,3	-127,4	-276,1	155,0	435,2
1550	1600	1575	95,5	387,5	2268	-1233	1035	216,7	927,9	-117,8	-393,9	98,9	534,1
1500	1550	1525	87,8	475,3	2170	-1376	794	190,5	1118,4	-120,8	-514,7	69,7	603,8
1450	1500	1475	73,7	549,0	2073	-1537	536	152,9	1271,4	-113,4	-628,0	39,6	643,3
1400	1450	1425	61,2	610,2	1962	-1739	222	120,1	1391,5	-106,5	-734,5	13,6	657,0
1350	1400	1375	49,4	659,6	1832	-2006	-173	90,6	1482,1	-99,2	-833,7	-8,6	648,4
1300	1350	1325	36,5	696,1	1706	-2294	-588	62,3	1544,4	-83,8	-917,5	-21,5	626,9
1250	1300	1275	39,7	735,8	1582	-2600	-1018	62,9	1607,2	-103,3	-1020,8	-40,5	586,5
1200	1250	1225	44,5	780,3	1437	-2976	-1538	63,9	1671,2	-132,3	-1153,1	-68,4	518,0
1150	1200	1175	45,2	825,5	1280	-3397	-2116	57,9	1729,1	-153,6	-1306,7	-95,7	422,4
1100	1150	1125	42,9	868,4	1162	-3781	-2618	49,9	1779,0	-162,4	-1469,1	-112,4	309,9
1050	1100	1075	31,3	899,7	1054	-4094	-3040	33,0	1812,0	-128,1	-1597,1	-95,1	214,8
1000	1050	1025	32,4	932,1	955	-4366	-3410	31,0	1842,9	-141,5	-1738,6	-110,5	104,3
950	1000	975	29,8	961,9	794	-4736	-3942	23,6	1866,6	-140,9	-1879,5	-117,3	-13,0
900	950	925	25,0	986,9	602	-5120	-4518	15,1	1881,6	-128,1	-2007,6	-113,0	-126,0
850	900	875	22,9	1009,8	441	-5419	-4977	10,1	1891,8	-124,3	-2131,9	-114,1	-240,1
800	850	825	18,2	1028,0	311	-5655	-5344	5,7	1897,4	-103,1	-2235,0	-97,4	-337,6
750	800	775	9,9	1037,9	219	-5803	-5583	2,2	1899,6	-57,2	-2292,2	-55,1	-392,6
700	750	725	0,2	1038,1	164	-5863	-5699	0,0	1899,6	-1,2	-2293,4	-1,2	-393,8

Brúarjökull

Elevation (m a.s.l.)			ΔS (km^2)	∑ΔS (km^2)	b_w (mm)	b_s (mm)	b_n (mm)	ΔB_w ($10^6 m^3$)	$\sum\Delta B_w$ ($10^6 m^3$)	ΔB_s ($10^6 m^3$)	$\sum\Delta B_s$ ($10^6 m^3$)	ΔB_n ($10^6 m^3$)	$\sum B_n$ ($10^6 m^3$)
1850	1900	1875	1,2	1,2	2470	-657	1812	2,9	3,0	-0,8	-0,8	2,2	2,2
1800	1850	1825	4,4	5,6	2563	-507	2056	11,3	14,3	-2,2	-3,1	9,1	11,3
1750	1800	1775	2,9	8,5	2543	-603	1939	7,3	21,6	-1,7	-4,8	5,5	16,8
1700	1750	1725	3,9	12,4	2513	-720	1793	9,9	31,5	-2,8	-7,6	7,0	23,9
1650	1700	1675	5,5	17,9	2487	-817	1670	13,7	45,2	-4,5	-12,1	9,2	33,1
1600	1650	1625	50,9	68,8	2424	-1073	1351	123,5	168,6	-54,6	-66,7	68,9	101,9
1550	1600	1575	46,0	114,8	2455	-1143	1312	112,9	281,6	-52,6	-119,3	60,3	162,2
1500	1550	1525	72,6	187,4	2410	-1215	1194	174,9	456,5	-88,2	-207,6	86,7	248,9
1450	1500	1475	78,3	265,7	2417	-1316	1100	189,3	645,7	-103,1	-310,7	86,2	335,1
1400	1450	1425	111,1	376,8	2686	-1376	1310	298,4	944,2	-152,9	-463,5	145,5	480,6
1350	1400	1375	155,7	532,5	2608	-1453	1154	406,2	1350,4	-226,4	-689,9	179,8	660,5
1300	1350	1325	147,1	679,6	2384	-1574	809	350,9	1701,3	-231,7	-921,7	119,2	779,6
1250	1300	1275	141,8	821,4	2165	-1742	423	307,2	2008,4	-247,1	-1168,8	60,1	839,7
1200	1250	1225	117,9	939,3	1899	-1923	-23	224,0	2232,4	-226,8	-1395,5	-2,8	836,9
1150	1200	1175	102,7	1042,0	1634	-2117	-482	167,9	2400,3	-217,4	-1613,0	-49,6	787,3
1100	1150	1125	83,4	1125,4	1365	-2339	-974	113,9	2514,2	-195,2	-1808,1	-81,3	706,0
1050	1100	1075	69,8	1195,2	1142	-2587	-1444	79,8	2593,9	-180,6	-1988,7	-100,8	605,2
1000	1050	1025	62,5	1257,7	937	-2904	-1967	58,5	2652,5	-181,5	-2170,2	-122,9	482,3
950	1000	975	56,4	1314,1	742	-3290	-2547	41,9	2694,3	-185,5	-2355,7	-143,6	338,7
900	950	925	46,3	1360,4	572	-3721	-3148	26,5	2720,9	-172,3	-2528,0	-145,8	192,9
850	900	875	42,2	1402,6	411	-4167	-3755	17,4	2738,2	-176,1	-2704,0	-158,7	34,2
800	850	825	36,4	1439,0	267	-4592	-4325	9,7	2748,0	-167,1	-2871,1	-157,4	-123,1
750	800	775	34,2	1473,2	125	-5214	-5088	4,3	2752,3	-178,3	-3049,4	-174,0	-297,1
700	750	725	22,1	1495,3	33	-5814	-5781	0,7	2753,0	-128,7	-3178,1	-128,0	-425,1
650	700	675	5,0	1500,3	-52	-6124	-6177	-0,3	2752,7	-30,5	-3208,6	-30,8	-455,9
600	650	625	0,0	1500,3	-117	-6351	-6468	0,0	2752,7	0,0	-3208,7	0,0	-455,9

Eyjabakkajökull

Elevation (m a.s.l.)			ΔS (km^2)	∑ΔS (km^2)	b_w (mm)	b_s (mm)	b_n (mm)	ΔB_w ($10^6 m^3$)	$\sum\Delta B_w$ ($10^6 m^3$)	ΔB_s ($10^6 m^3$)	$\sum\Delta B_s$ ($10^6 m^3$)	ΔB_n ($10^6 m^3$)	$\sum B_n$ ($10^6 m^3$)
1550	1600	1575	0,0	0,0	3248	-1138	2110	0,0	0,0	0,0	0,0	0,0	0,0
1500	1550	1525	0,0	0,0	3245	-1130	2115	0,3	0,3	-0,1	-0,1	0,2	0,2
1450	1500	1475	1,0	1,0	3156	-1213	1943	3,1	3,4	-1,2	-1,3	1,9	2,1
1400	1450	1425	1,8	2,8	3140	-1251	1889	5,8	9,2	-2,3	-3,6	3,5	5,6
1350	1400	1375	2,5	5,3	3054	-1354	1700	7,7	16,9	-3,4	-7,0	4,3	9,9
1300	1350	1325	4,1	9,4	2995	-1470	1525	12,3	29,1	-6,0	-13,0	6,3	16,1
1250	1300	1275	13,7	23,1	2753	-1697	1055	37,8	66,9	-23,3	-36,3	14,5	30,6
1200	1250	1225	13,4	36,5	2415	-1903	511	32,3	99,2	-25,5	-61,8	6,8	37,4
1150	1200	1175	14,4	50,9	2049	-2083	-34	29,4	128,7	-29,9	-91,7	-0,5	36,9
1100	1150	1125	12,1	63,0	1790	-2347	-556	21,7	150,4	-28,4	-120,2	-6,7	30,2
1050	1100	1075	10,4	73,4	1509	-2647	-1138	15,7	166,0	-27,5	-147,6	-11,8	18,4
1000	1050	1025	10,0	83,4	1279	-2935	-1655	12,8	178,9	-29,4	-177,1	-16,6	1,8
950	1000	975	7,5	90,9	1086	-3262	-2176	8,2	187,0	-24,6	-201,6	-16,4	-14,6
900	950	925	4,9	95,8	915	-3671	-2756	4,5	191,5	-18,0	-219,7	-13,5	-28,1
850	900	875	3,9	99,7	774	-4042	-3267	3,1	194,6	-15,9	-235,6	-12,9	-41,0
800	850	825	2,8	102,5	538	-4429	-3891	1,5	196,1	-12,3	-247,9	-10,8	-51,8
750	800	775	2,4	104,9	222	-4978	-4756	0,5	196,6	-11,7	-259,6	-11,2	-63,0
700	750	725	2,1	107,0	49	-5448	-5398	0,1	196,7	-11,4	-271,1	-11,3	-74,4
650	700	675	0,7	107,7	-11	-5657	-5669	0,0	196,7	-4,0	-275,1	-4,0	-78,4

Hoffellsjökull

Elevation (m a.s.l.)			ΔS (km^2)	∑ΔS (km^2)	b_w (mm)	b_s (mm)	b_n (mm)	ΔB_w ($10^6 m^3$)	$\sum\Delta B_w$ ($10^6 m^3$)	ΔB_s ($10^6 m^3$)	$\sum\Delta B_s$ ($10^6 m^3$)	ΔB_n ($10^6 m^3$)	$\sum B_n$ ($10^6 m^3$)
1450	1500	1475	0,9	0,9	3167	-1199	1967	2,9	2,9	-1,1	-1,1	1,8	1,8
1400	1450	1425	7,2	8,1	3385	-1216	2168	24,4	27,3	-8,8	-9,9	15,6	17,4
1350	1400	1375	10,2	18,3	3268	-1314	1954	33,2	60,5	-13,4	-23,2	19,9	37,3
1300	1350	1325	16,3	34,6	3153	-1518	1635	51,4	111,9	-24,7	-48,0	26,6	63,9
1250	1300	1275	34,9	69,5	2964	-1772	1191	103,5	215,4	-61,9	-109,9	41,6	105,5
1200	1250	1225	25,8	95,3	3016	-1978	1038	77,9	293,3	-51,1	-161,0	26,8	132,4
1150	1200	1175	17,9	113,2	2990	-2265	725	53,7	347,0	-40,6	-201,6	13,0	145,4
1100	1150	1125	16,9	130,1	2846	-2644	201	48,0	395,0	-44,6	-246,3	3,4	148,8
1050	1100	1075	12,7	142,8	2590	-3123	-532	32,8	427,9	-39,6	-285,8	-6,8	142,0
1000	1050	1025	9,6	152,4	2332	-3561	-1229	22,3	450,2	-34,1	-319,9	-11,8	130,3
950	1000	975	8,7	161,1	2031	-3951	-1919	17,6	467,7	-34,2	-354,1	-16,6	113,7
900	950	925	6,4	167,5	1716	-4327	-2610	11,0	478,7	-27,7	-381,8	-16,7	96,9
850	900	875	4,3	171,8	1454	-4650	-3196	6,2	484,9	-19,8	-401,6	-13,6	83,3
800	850	825	3,4	175,2	1236	-4737	-3501	4,2	489,1	-16,0	-417,7	-11,8	71,5
750	800	775	3,8	179,0	975	-4985	-4009	3,8	492,9	-19,2	-436,8	-15,4	56,0
700	750	725	3,5	182,5	756	-5240	-4483	2,7	495,5	-18,4	-455,3	-15,8	40,2
650	700	675	3,4	185,9	545	-5564	-5019	1,9	497,4	-19,0	-474,3	-17,1	23,1
600	650	625	2,5	188,4	301	-5919	-5618	0,7	498,2	-14,6	-488,9	-13,9	9,3
550	600	575	1,6	190,0	9	-6240	-6231	0,0	498,2	-10,1	-499,0	-10,1	-0,8
500	550	525	1,5	191,5	-391	-6540	-6932	-0,6	497,6	-9,7	-508,8	-10,3	-11,2
450	500	475	0,8	192,3	-791	-6822	-7613	-0,6	497,0	-5,4	-514,1	-6,0	-17,2
400	450	425	0,9	193,2	-1146	-7105	-8252	-1,0	495,9	-6,3	-520,5	-7,3	-24,5
350	400	375	0,6	193,8	-1417	-7313	-8730	-0,8	495,1	-4,3	-524,8	-5,2	-29,7
300	350	325	0,7	194,5	-1636	-7446	-9082	-1,1	494,0	-5,1	-529,8	-6,2	-35,9
250	300	275	1,3	195,8	-1842	-7607	-9450	-2,4	491,6	-9,9	-539,7	-12,3	-48,1
200	250	225	2,6	198,4	-2110	-8153	-10264	-5,4	486,1	-21,0	-560,8	-26,5	-74,6
150	200	175	2,9	201,3	-2416	-9752	-12168	-7,0	479,1	-28,4	-589,1	-35,4	-110,0
100	150	125	2,1	203,4	-2609	-10733	-13343	-5,6	473,6	-22,9	-612,0	-28,4	-138,5
50	100	75	1,4	204,8	-2725	-11136	-13861	-3,9	469,7	-15,9	-627,9	-19,8	-158,3
0	50	25	1,0	205,8	-2766	-11491	-14257	-2,7	467,0	-11,1	-639,1	-13,8	-172,1

Breiðamerkurjökull

Elevation (m a.s.l.)			ΔS (km^2)	∑ΔS (km^2)	b_w (mm)	b_s (mm)	b_n (mm)	ΔB_w ($10^6 m^3$)	$\sum\Delta B_w$ ($10^6 m^3$)	ΔB_s ($10^6 m^3$)	$\sum\Delta B_s$ ($10^6 m^3$)	ΔB_n ($10^6 m^3$)	$\sum B_n$ ($10^6 m^3$)
1900	1950	1925	0,0	0,0	6113	-345	5767	0,5	0,5	0,0	0,0	0,5	0,5
1850	1900	1875	0,4	0,4	6096	-376	5719	2,3	2,7	-0,1	-0,2	2,1	2,6
1800	1850	1825	0,5	0,9	5979	-449	5530	2,8	5,6	-0,2	-0,4	2,6	5,2
1750	1800	1775	1,0	1,9	5604	-623	4981	5,6	11,2	-0,6	-1,0	5,0	10,2
1700	1750	1725	2,6	4,5	4228	-914	3314	11,1	22,2	-2,4	-3,4	8,7	18,8
1650	1700	1675	6,0	10,5	3419	-978	2441	20,5	42,7	-5,9	-9,3	14,6	33,5
1600	1650	1625	17,2	27,7	2996	-1044	1952	51,4	94,1	-17,9	-27,2	33,5	66,9
1550	1600	1575	26,0	53,7	2813	-1131	1682	73,0	167,2	-29,4	-56,5	43,7	110,6
1500	1550	1525	32,0	85,7	2729	-1312	1417	87,3	254,4	-41,9	-98,5	45,3	155,9
1450	1500	1475	45,9	131,6	2790	-1410	1380	128,2	382,6	-64,8	-163,3	63,4	219,3
1400	1450	1425	59,2	190,8	2703	-1515	1187	160,1	542,8	-89,8	-253,1	70,4	289,7
1350	1400	1375	89,4	280,2	2625	-1653	972	234,8	777,6	-147,9	-400,9	87,0	376,6
1300	1350	1325	95,2	375,4	2413	-1855	557	229,7	1007,3	-176,6	-577,5	53,1	429,7
1250	1300	1275	57,6	433,0	2248	-2064	183	129,5	1136,7	-118,9	-696,4	10,6	440,3
1200	1250	1225	39,7	472,7	2135	-2313	-178	84,8	1221,6	-91,9	-788,4	-7,1	433,2
1150	1200	1175	31,7	504,4	1973	-2597	-624	62,6	1284,2	-82,4	-870,8	-19,8	413,4
1100	1150	1125	27,3	531,7	1796	-2944	-1148	49,0	1333,2	-80,3	-951,1	-31,3	382,1
1050	1100	1075	23,8	555,5	1592	-3277	-1684	37,9	1371,1	-77,9	-1029,1	-40,1	342,0
1000	1050	1025	21,9	577,4	1411	-3552	-2140	30,9	1402,0	-77,7	-1106,8	-46,8	295,2
950	1000	975	24,4	601,8	1187	-3852	-2664	28,9	1430,9	-93,8	-1200,6	-64,9	230,3
900	950	925	27,1	628,9	1032	-4059	-3027	27,9	1458,8	-109,9	-1310,5	-82,0	148,4
850	900	875	25,4	654,3	864	-4369	-3504	22,0	1480,8	-111,1	-1421,6	-89,1	59,2
800	850	825	25,7	680,0	670	-4710	-4039	17,2	1498,0	-120,9	-1542,5	-103,7	-44,5
750	800	775	25,1	705,1	437	-5107	-4670	11,0	1509,0	-128,2	-1670,7	-117,2	-161,7
700	750	725	22,2	727,3	273	-5372	-5099	6,1	1515,1	-119,1	-1789,7	-113,0	-274,7
650	700	675	31,3	758,6	136	-5531	-5394	4,3	1519,3	-173,1	-1962,8	-168,8	-443,5
600	650	625	25,5	784,1	-200	-5902	-6102	-5,1	1514,2	-150,7	-2113,6	-155,9	-599,4
550	600	575	26,8	810,9	-657	-6285	-6942	-17,6	1496,6	-168,2	-2281,8	-185,8	-785,1
500	550	525	15,5	826,4	-974	-6540	-7514	-15,1	1481,5	-101,3	-2383,1	-116,4	-901,5
450	500	475	14,5	840,9	-1513	-6877	-8391	-22,0	1459,5	-99,9	-2483,0	-121,9	-1023,5
400	450	425	16,4	857,3	-1888	-7120	-9009	-31,0	1428,5	-116,9	-2599,9	-147,9	-1171,4
350	400	375	13,0	870,3	-2242	-7336	-9579	-29,1	1399,4	-95,2	-2695,2	-124,3	-1295,7
300	350	325	11,3	881,6	-2414	-7477	-9891	-27,4	1372,0	-84,8	-2780,0	-112,2	-1407,9
250	300	275	11,1	892,7	-2536	-7667	-10203	-28,1	1344,0	-84,9	-2864,8	-113,0	-1520,9
200	250	225	11,4	904,1	-2631	-8190	-10821	-29,9	1314,1	-93,0	-2957,8	-122,8	-1643,7
150	200	175	9,3	913,4	-2752	-9835	-12588	-25,7	1288,4	-91,8	-3049,6	-117,5	-1761,2
100	150	125	7,7	921,1	-2882	-11127	-14010	-22,2	1266,2	-85,6	-3135,1	-107,7	-1868,9
50	100	75	3,8	924,9	-2960	-11690	-14651	-11,2	1255,0	-44,2	-3179,3	-55,4	-1924,3
0	50	25	0,0	924,9	-3012	-11781	-14793	-0,3	1254,8	-1,1	-3180,4	-1,3	-1925,6

Síðujökull

Elevation (m a.s.l.)			ΔS (km^2)	∑ΔS (km^2)	b_w (mm)	b_s (mm)	b_n (mm)	ΔB_w ($10^6 m^3$)	$\sum\Delta B_w$ ($10^6 m^3$)	ΔB_s ($10^6 m^3$)	$\sum\Delta B_s$ ($10^6 m^3$)	ΔB_n ($10^6 m^3$)	$\sum B_n$ ($10^6 m^3$)
1700	1750	1725	0,8	0,8	3493	-1223	2269	2,9	2,9	-1,0	-1,0	1,9	1,9
1650	1700	1675	5,5	6,3	3167	-1193	1973	17,5	20,5	-6,6	-7,6	10,9	12,8
1600	1650	1625	11,1	17,4	2841	-1220	1621	31,5	52,0	-13,5	-21,2	18,0	30,8
1550	1600	1575	10,7	28,1	2833	-1285	1548	30,4	82,4	-13,8	-35,0	16,6	47,4
1500	1550	1525	20,5	48,6	2815	-1327	1488	57,6	140,0	-27,2	-62,1	30,4	77,9
1450	1500	1475	39,0	87,6	2643	-1628	1014	103,2	243,2	-63,6	-125,7	39,6	117,5
1400	1450	1425	25,9	113,5	2475	-2068	407	64,1	307,3	-53,6	-179,3	10,6	128,0
1350	1400	1375	21,2	134,7	2278	-2496	-217	48,2	355,6	-52,9	-232,1	-4,6	123,4
1300	1350	1325	17,3	152,0	2072	-2853	-780	35,9	391,5	-49,4	-281,5	-13,5	109,9
1250	1300	1275	15,9	167,9	1920	-3144	-1223	30,6	422,0	-50,1	-331,6	-19,5	90,4
1200	1250	1225	21,1	189,0	1801	-3431	-1630	38,1	460,1	-72,5	-404,1	-34,4	56,0
1150	1200	1175	18,3	207,3	1642	-3764	-2121	30,0	490,1	-68,7	-472,8	-38,7	17,3
1100	1150	1125	17,2	224,5	1489	-3887	-2397	25,7	515,7	-67,0	-539,8	-41,3	-24,1
1050	1100	1075	16,2	240,7	1365	-4068	-2703	22,1	537,9	-66,0	-605,8	-43,8	-67,9
1000	1050	1025	20,5	261,2	1222	-4533	-3310	25,1	563,0	-93,0	-698,7	-67,9	-135,8
950	1000	975	20,2	281,4	990	-4947	-3957	20,0	582,9	-99,8	-798,5	-79,8	-215,6
900	950	925	21,6	303,0	722	-5135	-4413	15,6	598,5	-110,8	-909,3	-95,2	-310,8
850	900	875	19,7	322,7	523	-5287	-4763	10,3	608,8	-104,0	-1013,3	-93,7	-404,5
800	850	825	20,9	343,6	337	-5545	-5207	7,1	615,9	-115,9	-1129,2	-108,9	-513,3
750	800	775	22,7	366,3	139	-5962	-5822	3,2	619,0	-135,2	-1264,4	-132,0	-645,3
700	750	725	23,1	389,4	-52	-6432	-6485	-1,2	617,8	-148,5	-1412,9	-149,8	-795,1
650	700	675	18,4	407,8	-246	-6859	-7105	-4,5	613,3	-126,3	-1539,2	-130,8	-925,9
600	650	625	3,8	411,6	-378	-7115	-7493	-1,4	611,8	-27,0	-1566,2	-28,5	-954,4

Skaftárjökull

Elevation (m a.s.l.)			ΔS (km^2)	∑ΔS (km^2)	b_w (mm)	b_s (mm)	b_n (mm)	ΔB_w ($10^6 m^3$)	$\sum\Delta B_w$ ($10^6 m^3$)	ΔB_s ($10^6 m^3$)	$\sum\Delta B_s$ ($10^6 m^3$)	ΔB_n ($10^6 m^3$)	$\sum B_n$ ($10^6 m^3$)
1350	1400	1375	2,3	2,3	2135	-2535	-399	5,0	5,0	-5,9	-5,9	-0,9	-0,9
1300	1350	1325	5,4	7,7	1949	-2845	-896	10,4	15,4	-15,2	-21,2	-4,8	-5,7
1250	1300	1275	4,2	11,9	1831	-3195	-1363	7,8	23,2	-13,5	-34,7	-5,8	-11,5
1200	1250	1225	6,5	18,4	1728	-3532	-1803	11,2	34,4	-22,9	-57,6	-11,7	-23,2
1150	1200	1175	7,9	26,3	1609	-3765	-2156	12,7	47,1	-29,7	-87,3	-17,0	-40,2
1100	1150	1125	11,2	37,5	1467	-3863	-2396	16,4	63,4	-43,1	-130,4	-26,7	-66,9
1050	1100	1075	12,9	50,4	1283	-3967	-2683	16,6	80,0	-51,3	-181,6	-34,7	-101,6
1000	1050	1025	12,9	63,3	1092	-4354	-3262	14,1	94,2	-56,4	-238,0	-42,2	-143,8
950	1000	975	8,5	71,8	877	-4832	-3954	7,5	101,6	-41,2	-279,1	-33,7	-177,5
900	950	925	5,5	77,3	697	-5175	-4478	3,8	105,5	-28,3	-307,4	-24,5	-202,0
850	900	875	5,3	82,6	517	-5474	-4956	2,8	108,2	-29,2	-336,7	-26,5	-228,5
800	850	825	5,0	87,6	339	-5774	-5434	1,7	109,9	-28,6	-365,3	-26,9	-255,4
750	800	775	4,6	92,2	157	-6028	-5871	0,7	110,6	-28,0	-393,2	-27,2	-282,6
700	750	725	4,3	96,5	-23	-6426	-6450	-0,1	110,5	-27,4	-420,7	-27,5	-310,1
650	700	675	1,6	98,1	-165	-6854	-7020	-0,3	110,3	-11,0	-431,6	-11,2	-321,4
600	650	625	0,0	98,1	-262	-7643	-7905	0,0	110,3	0,0	-431,7	0,0	-321,5

Vestari Skaftárketill

Elevation (m a.s.l.)			ΔS (km^2)	∑ΔS (km^2)	b_w (mm)	b_s (mm)	b_n (mm)	ΔB_w ($10^6 m^3$)	$\sum\Delta B_w$ ($10^6 m^3$)	ΔB_s ($10^6 m^3$)	$\sum\Delta B_s$ ($10^6 m^3$)	ΔB_n ($10^6 m^3$)	$\sum B_n$ ($10^6 m^3$)
1900	1950	1925	0,6	0,6	2535	-648	1887	1,4	1,4	-0,4	-0,4	1,1	1,1
1850	1900	1875	0,6	1,2	2520	-685	1835	1,6	3,0	-0,4	-0,8	1,1	2,2
1800	1850	1825	0,8	2,0	2490	-710	1779	1,9	4,9	-0,5	-1,3	1,4	3,6
1750	1800	1775	2,6	4,6	2375	-790	1584	6,1	11,0	-2,0	-3,4	4,1	7,7
1700	1750	1725	5,5	10,1	2249	-923	1325	12,4	23,5	-5,1	-8,5	7,3	15,0
1650	1700	1675	6,6	16,7	2147	-1142	1004	14,2	37,7	-7,6	-16,1	6,7	21,6
1600	1650	1625	7,6	24,3	2097	-1264	833	15,9	53,6	-9,6	-25,7	6,3	28,0
1550	1600	1575	5,5	29,8	2036	-1345	691	11,1	64,8	-7,4	-33,0	3,8	31,8
1500	1550	1525	1,5	31,3	2013	-1358	654	3,1	67,8	-2,1	-35,1	1,0	32,8

Eystri Skaftárketill

Elevation (m a.s.l.)			ΔS (km^2)	∑ΔS (km^2)	b_w (mm)	b_s (mm)	b_n (mm)	ΔB_w ($10^6 m^3$)	$\sum\Delta B_w$ ($10^6 m^3$)	ΔB_s ($10^6 m^3$)	$\sum\Delta B_s$ ($10^6 m^3$)	ΔB_n ($10^6 m^3$)	$\sum B_n$ ($10^6 m^3$)
1750	1800	1775	1,1	1,1	2343	-826	1517	2,5	2,5	-0,9	-0,9	1,6	1,6
1700	1750	1725	10,2	11,3	2286	-905	1381	23,3	25,8	-9,2	-10,1	14,1	15,7
1650	1700	1675	16,5	27,8	2281	-993	1288	37,7	63,5	-16,4	-26,5	21,3	37,0
1600	1650	1625	9,7	37,5	2236	-1102	1134	21,6	85,1	-10,6	-37,2	10,9	48,0
1550	1600	1575	2,4	39,9	2229	-1121	1107	5,4	90,5	-2,7	-39,9	2,7	50,6

Gjálp

Elevation (m a.s.l.)			ΔS (km^2)	∑ΔS (km^2)	b_w (mm)	b_s (mm)	b_n (mm)	ΔB_w ($10^6 m^3$)	$\sum\Delta B_w$ ($10^6 m^3$)	ΔB_s ($10^6 m^3$)	$\sum\Delta B_s$ ($10^6 m^3$)	ΔB_n ($10^6 m^3$)	$\sum B_n$ ($10^6 m^3$)
1900	1950	1925	0,4	0,4	2541	-649	1892	1,0	1,0	-0,2	-0,2	0,7	0,7
1850	1900	1875	0,7	1,1	2523	-708	1814	1,8	2,8	-0,5	-0,8	1,3	2,0
1800	1850	1825	1,1	2,2	2492	-754	1737	2,8	5,6	-0,9	-1,6	2,0	4,0
1750	1800	1775	4,9	7,1	2374	-831	1543	11,5	17,2	-4,0	-5,7	7,5	11,5
1700	1750	1725	18,8	25,9	2396	-878	1518	45,0	62,1	-16,5	-22,1	28,5	40,0
1650	1700	1675	13,5	39,4	2432	-894	1538	32,8	95,0	-12,1	-34,2	20,8	60,8

Grímsvötn

Elevation (m a.s.l.)			ΔS (km^2)	∑ΔS (km^2)	b_w (mm)	b_s (mm)	b_n (mm)	ΔB_w ($10^6 m^3$)	$\sum\Delta B_w$ ($10^6 m^3$)	ΔB_s ($10^6 m^3$)	$\sum\Delta B_s$ ($10^6 m^3$)	ΔB_n ($10^6 m^3$)	$\sum B_n$ ($10^6 m^3$)
1700	1750	1725	0,7	0,7	2479	-915	1564	1,8	1,8	-0,7	-0,7	1,2	1,2
1650	1700	1675	40,6	41,3	2484	-1016	1467	100,9	102,7	-41,3	-42,0	59,6	60,7
1600	1650	1625	30,8	72,1	2482	-1169	1312	76,5	179,2	-36,0	-78,0	40,4	101,2
1550	1600	1575	19,2	91,3	2482	-1261	1221	47,7	226,9	-24,2	-102,2	23,5	124,6
1500	1550	1525	16,9	108,2	2483	-1419	1063	42,0	268,9	-24,0	-126,2	18,0	142,6
1450	1500	1475	10,0	118,2	2503	-1711	791	25,1	294,0	-17,2	-143,4	7,9	150,6
1400	1450	1425	11,7	129,9	2552	-2101	450	29,8	323,8	-24,6	-168,0	5,3	155,8
1350	1400	1375	4,3	134,2	2603	-2131	472	11,3	335,1	-9,2	-177,2	2,0	157,9
1300	1350	1325	0,7	134,9	2715	-2020	695	2,0	337,2	-1,5	-178,7	0,5	158,4

Appendix C: Coordinates of the velocity measurement stakes in 2019.

Position of the velocity measurement stakes determined by GPS sub-metre differential (I), fast static (FS) and kinematic (K). (Accuracy of horizontal position 0.5 – 1.0 m, and vertical accuracy 1-2 m for DGPS, about 1cm for fast static, and 3 cm for kinematic).
The station Hofn in Höfn í Hornafirði is used as a stationary reference for all measurements, ÍSN93 datum, h_l is elevation above ellipsoid, dL antenna height, N estimated difference between ellipsoid and sea-level, H elevation in metres above sea level ($H= h_l+N+dL$). X and Y are ÍSN93 Lambert conformal conic projected coordinates. M is a quality marker.

Site	time	Date	Calender Day #	Year		Latitude		Longitude	h_l (m a. e.)	dL (m)	N (m)	H (m a. s. l.)	X	Y	M
B07-19	14,522	1	5	121	2019	64	25,80052	16	17,46419	1426,8	0,0	-67,1	1359,7	630467,24	439252,79	K
B07-19	17,897	18	10	291	2019	64	25,79963	16	17,46375	1424,5	-1,6	-67,1	1355,8	630467,67	439251,14	K
B09-19	13,316	3	5	123	2019	64	44,84373	16	5,85773	791,6	0,0	-66,7	724,9	638153,53	475011,21	K
B09-19	17,147	19	10	292	2019	64	44,84455	16	5,85663	785,7	0,0	-66,7	719,1	638154,33	475012,77	K
B10-19	12,522	3	5	123	2019	64	43,68734	16	6,69863	846,0	0,0	-66,7	779,3	637585,01	472834,32	K
B10-19	16,197	19	10	292	2019	64	43,68752	16	6,69944	841,0	0,0	-66,7	774,3	637584,36	472834,63	K
B11-19	10,703	3	5	123	2019	64	40,96873	16	10,45338	1016,9	0,0	-66,8	950,0	634831,81	467653,46	K
B11-19	16,005	19	10	292	2019	64	40,97387	16	10,44917	1013,6	0,0	-66,8	946,7	634834,73	467663,16	K
B12-19	9,929	3	5	123	2019	64	38,26132	16	14,13586	1144,4	0,0	-66,9	1077,5	632125,11	462498,43	K
B12-19	15,343	19	10	292	2019	64	38,27537	16	14,12337	1142,3	0,0	-66,9	1075,4	632133,91	462524,94	K
B13-19	17,155	19	10	292	2019	64	34,54287	16	19,69090	1285,3	0,0	-67,0	1218,2	627994,63	455405,47	K
B13ror15	16,071	3	5	123	2019	64	34,58820	16	19,65560	1287,1	-1,8	-67,0	1218,2	628019,24	455490,80	K
B13ror15	16,341	19	10	292	2019	64	34,60590	16	19,63398	1285,6	0,0	-67,0	1218,6	628035,10	455524,39	K
B14-19	17,797	3	5	123	2019	64	31,64359	16	24,70416	1389,6	0,0	-67,1	1322,4	624214,69	449856,60	K
B14-19	18,536	19	10	292	2019	64	31,65700	16	24,68084	1384,9	0,0	-67,1	1317,8	624232,31	449882,26	K
B15-19	18,459	3	5	123	2019	64	28,49176	16	30,02502	1473,0	0,0	-67,2	1405,8	620192,50	443833,83	K
B15-19	19,252	19	10	292	2019	64	28,49832	16	30,00932	1468,0	0,0	-67,2	1400,7	620204,59	443846,51	K
B16-19	14,411	30	5	150	2019	64	24,12909	16	40,87766	1596,2	0,0	-67,9	1528,4	611796,30	435401,98	K
B16-19	20,584	19	10	292	2019	64	24,12951	16	40,87796	1594,1	0,0	-67,3	1526,7	611796,04	435402,76	K
B17-19	15,429	3	5	123	2019	64	36,73425	16	28,79375	1284,0	0,0	-67,1	1216,9	620568,40	459175,36	K
B17-19	15,634	19	10	292	2019	64	36,75127	16	28,78178	1281,5	0,0	-67,1	1214,4	620576,68	459207,33	K
B18-19	17,025	1	5	121	2019	64	31,57711	16	0,13977	1383,1	0,0	-66,9	1316,2	643854,85	450601,24	K
B18-19	18,248	18	10	291	2019	64	31,58318	16	0,14348	1381,3	-1,8	-66,9	1312,6	643851,35	450612,36	K
B19-19	16,202	1	5	121	2019	64	27,99765	15	55,98587	1508,3	0,0	-66,9	1441,4	647497,15	444117,81	K
B19-19	18,432	18	10	291	2019	64	27,99801	15	55,98653	1503,2	0,0	-66,9	1436,3	647496,59	444118,44	K
BB0-19	14,514	1	5	121	2019	64	22,71071	16	5,05241	1588,6	0,0	-66,9	1521,8	640688,04	433961,24	K
BB0-19	16,383	18	10	291	2019	64	22,71056	16	5,05416	1583,7	0,0	-66,9	1516,8	640686,65	433960,89	K
Barc-19	14,359	1	6	152	2019	64	38,40904	17	26,77970	1962,8	0,0	-67,9	1894,9	574267,47	460796,27	K
Bor-19	16,885	6	6	157	2019	64	24,94002	17	20,13878	1473,2	-0,4	-67,7	1405,1	580215,81	435914,21	K
Bor-19	11,300	30	8	241	2019	64	24,93677	17	20,14262	1491,2	-1,6	-67,7	1421,9	580212,88	435908,09	K
Bor-19	13,331	22	10	295	2019	64	24,93258	17	20,14311	1500,3	-1,7	-67,7	1430,8	580212,70	435900,31	K
Borth-17	17,000	5	3	64	2019	64	25,04412	17	19,17962	1478,6	0,0	-67,7	1406,0	580980,95	436127,96	K
Borth-19	14,600	8	6	159	2019	64	25,04428	17	19,17892	1476,5	-1,3	-67,7	1407,6	580981,51	436128,25	K
Borth-19	10,950	30	8	241	2019	64	25,04057	17	19,17963	1496,6	-1,6	-67,7	1427,3	580981,12	436121,35	K
Borth-19	14,627	22	10	295	2019	64	25,03880	17	19,17908	1507,7	-2,8	-67,7	1437,2	580981,10	436118,01	K
Br1-19	18,557	3	4	94	2019	64	5,83673	16	19,71068	170,0	0,0	-65,9	104,1	630232,12	402116,03	K
Br1-19	10,476	27	11	331	2019	64	5,83633	16	19,71177	157,6	-0,2	-65,9	91,6	630231,26	402115,26	K
Br1-20	12,527	27	11	331	2019	64	5,96256	16	19,82037	180,9	-0,2	-65,9	114,8	630133,19	402345,86	K
Br2-18	19,266	3	4	94	2019	64	6,36501	16	22,53387	258,1	0,0	-66,0	192,1	627899,00	403000,69	K
Br2-19	19,266	3	4	94	2019	64	6,36399	16	22,53387	258,1	0,0	-66,0	192,1	627899,00	402998,79	K
Br2-19	13,631	27	11	331	2019	64	6,36234	16	22,53361	248,8	-0,2	-66,0	182,5	627899,34	402995,73	K
Br3-18	11,143	4	4	95	2019	64	8,45566	16	24,02373	441,9	0,0	-66,3	375,6	626509,63	406831,80	K
Br3-19	11,143	4	4	95	2019	64	8,45388	16	24,02411	441,9	0,0	-66,3	375,6	626529,63	406828,60	K
Br3-19	12,194	28	11	332	2019	64	8,44655	16	24,01137	434,7	-0,5	-66,3	368,0	626540,52	406815,42	K
Br4-18	13,572	4	4	95	2019	64	10,78543	16	20,11857	579,2	0,0	-66,4	512,8	629513,45	411288,77	K
Br5-19	15,139	4	4	95	2019	64	13,55096	16	19,19915	744,4	0,0	-66,6	677,9	630040,02	416454,07	K
Br5-19	10,897	1	5	121	2019	64	13,53715	16	19,20069	743,2	0,0	-66,6	676,6	630039,86	416428,38	K

Br7-19	12,632	1	5	121	2019	64	22,16508	16	16,92697	1315,8	0,0	-67,0	1248,8	631188,52	432522,87	K
Br7-19	15,403	18	10	291	2019	64	22,13790	16	16,92054	1312,5	-2,4	-67,0	1243,0	631195,86	432472,65	K
Bru-19	17,908	2	5	122	2019	64	39,74819	15	56,54044	963,5	0,0	-66,8	896,7	645997,41	465903,21	K
Bru-19	10,056	19	10	292	2019	64	39,75763	15	56,53599	960,6	0,0	-66,8	893,8	646000,10	465920,88	K
Bud-19	17,183	2	5	122	2019	64	35,98939	15	59,89263	1205,0	0,0	-66,9	1138,2	643663,25	458799,39	K
Bud-19	19,526	18	10	291	2019	64	36,00159	15	59,88995	1201,1	0,0	-66,9	1134,2	643664,31	458822,12	K
D05-19	11,443	4	5	124	2019	64	42,22504	16	54,69678	1272,5	0,0	-67,4	1205,2	599585,25	468618,78	K
D05-19	14,015	20	10	293	2019	64	42,23658	16	54,68111	1268,4	0,0	-67,4	1201,0	599596,99	468640,61	K
D06GPS19	13,357	3	6	154	2019	64	40,45016	16	56,93510	1340,9	0,0	-67,4	1273,4	597913,94	465264,54	K
D06GPS19	13,388	20	10	293	2019	64	40,45990	16	56,92178	1338,0	0,0	-67,4	1270,6	597923,94	465282,97	K
D07-19	12,200	4	5	124	2019	64	38,28214	16	59,26243	1446,2	0,0	-67,5	1378,7	596191,08	461178,90	K
D07-19	12,967	20	10	293	2019	64	38,29811	16	59,24698	1441,3	0,0	-67,5	1373,8	596202,44	461208,96	K
D09-19	13,282	4	5	124	2019	64	31,79826	17	0,59711	1655,2	0,0	-67,6	1587,6	595507,27	449104,20	K
D09-19	11,302	20	10	293	2019	64	31,80217	17	0,59903	1651,4	0,0	-67,6	1583,8	595505,52	449111,40	K
D12-19	15,168	4	5	124	2019	64	28,97357	17	0,17719	1718,8	0,0	-67,6	1651,2	596008,82	443869,13	K
D12-19	12,529	20	10	293	2019	64	28,97382	17	0,17677	1714,9	0,0	-67,6	1647,4	596009,13	443869,61	K
E01-19	12,611	2	5	122	2019	64	40,62892	15	34,86367	832,9	0,0	-66,7	766,2	663143,43	468420,80	K
E01-19	12,911	19	10	292	2019	64	40,63186	15	34,86120	827,9	0,0	-66,7	761,2	663145,09	468426,37	K
E01-b	12,715	19	10	292	2019	64	40,63113	15	34,85639	828,0	0,0	-66,7	761,3	663148,99	468425,22	K
E01uav1a	13,205	19	10	292	2019	64	40,62820	15	34,85289	828,3	0,0	-66,7	761,6	663152,07	468419,93	K
E02-19	10,466	2	5	122	2019	64	39,12512	15	35,98533	1019,1	0,0	-66,8	952,3	662402,45	465582,68	K
E02-19	12,343	19	10	292	2019	64	39,13828	15	35,98062	1015,2	0,0	-66,8	948,5	662404,89	465607,29	K
E03-19	9,184	2	5	122	2019	64	36,66160	15	36,92523	1256,9	0,0	-66,9	1190,0	661899,92	460971,87	K
E03-19	11,620	19	10	292	2019	64	36,66688	15	36,92829	1251,9	0,0	-66,9	1185,1	661896,95	460981,53	K
E03-a2	12,008	19	10	292	2019	64	36,66769	15	36,91087	1252,0	0,0	-66,9	1185,2	661910,75	460983,78	K
E04-19	19,497	1	5	121	2019	64	34,95141	15	37,14840	1358,0	0,0	-66,8	1291,2	661892,02	457789,36	K
E04-19	12,676	19	10	292	2019	64	34,95222	15	37,14810	1353,0	0,0	-66,8	1286,1	661892,18	457790,89	K
Fl01-19	15,446	1	5	121	2019	64	26,15546	15	55,62360	1416,5	0,0	-66,8	1349,7	647953,61	440713,16	K
Fl01-19	17,299	18	10	291	2019	64	26,14857	15	55,60866	1410,5	0,0	-66,8	1343,6	647966,22	440700,95	K
G02-19	14,143	2	6	153	2019	64	26,84435	17	17,71632	1633,7	0,0	-67,7	1566,0	582065,83	439503,01	K
G02-19	11,683	20	10	293	2019	64	26,84006	17	17,72014	1633,3	-1,2	-67,7	1564,3	582062,99	439494,97	K
G03-19	13,422	2	6	153	2019	64	28,43541	17	16,33188	1727,7	0,0	-67,7	1660,0	583095,56	442488,25	K
G03-19	11,486	20	10	293	2019	64	28,43328	17	16,33373	1727,3	-1,7	-67,7	1657,8	583094,18	442484,26	K
G04-19	12,504	2	6	153	2019	64	30,01691	17	15,04780	1756,7	0,0	-67,7	1689,0	584043,26	445453,85	K
G04-19	12,879	20	10	293	2019	64	30,01684	17	15,04820	1756,3	-1,5	-67,7	1687,1	584042,95	445453,72	K
GeSig-19	13,200	31	5	151	2019	64	40,17562	16	41,05436	1674,5	-0,3	-67,3	1607,0	610562,46	465191,19	K
Go1-19	16,343	1	6	152	2019	64	33,97424	17	24,95507	1828,5	0,0	-67,8	1760,6	575927,28	452595,09	K
Go1-19	13,409	20	10	293	2019	64	33,97266	17	24,95478	1828,3	-1,7	-67,8	1758,8	575927,59	452592,16	K
Haab-19	17,879	6	6	157	2019	64	20,95983	17	24,11732	1800,4	-0,7	-67,5	1732,2	577207,57	428438,90	K
Haab-19	19,582	20	10	293	2019	64	20,96000	17	24,11800	1797,3	0,0	-67,5	1729,7	577207,02	428439,20	K
Hof01-19	18,630	1	5	121	2019	64	32,33577	15	35,84467	1211,2	0,0	-66,7	1144,5	663192,95	452992,38	K
Hof01-19	11,627	19	10	292	2019	64	32,32964	15	35,84437	1205,8	0,0	-66,7	1139,1	663193,80	452981,03	K
K01-19	11,846	5	5	125	2019	64	35,16936	17	51,83221	1116,7	0,0	-67,6	1049,1	554419,15	454353,31	K
K01-19	17,397	20	10	293	2019	64	35,17138	17	51,84200	1111,6	0,0	-67,6	1044,0	554411,28	454356,91	K
K02-19	11,172	5	5	125	2019	64	34,80678	17	49,67004	1240,9	0,0	-67,6	1173,3	556157,54	453711,26	K
K02-19	18,585	20	10	293	2019	64	34,81044	17	49,68647	1236,4	0,0	-67,6	1168,7	556144,30	453717,81	K
K03-19	10,904	5	5	125	2019	64	34,23717	17	46,39216	1364,1	0,0	-67,7	1296,4	558795,09	452702,79	K
K03-19	17,582	20	10	293	2019	64	34,24047	17	46,41442	1359,2	0,0	-67,7	1291,5	558777,20	452708,58	K
K04-19	13,346	5	5	125	2019	64	33,21109	17	42,24846	1557,0	0,0	-67,7	1489,3	562143,55	450862,78	K
K04-19	16,575	20	10	293	2019	64	33,21503	17	42,27507	1551,5	0,0	-67,7	1483,7	562122,14	450869,66	K
K05-19	13,879	5	5	125	2019	64	33,44615	17	35,45310	1749,4	0,0	-67,8	1681,6	567564,20	451415,60	K
K05-19	16,095	20	10	293	2019	64	33,44323	17	35,46807	1746,7	-1,8	-67,8	1677,1	567552,36	451409,91	K
K06-19pl	11,557	1	6	152	2019	64	38,34940	17	31,34875	2014,0	0,0	-67,9	1946,1	570630,63	460598,22	K
K06-19ve	12,705	1	6	152	2019	64	38,34859	17	31,34297	2014,0	0,0	-67,9	1946,1	570635,27	460596,83	K
K06-19ve	14,538	20	10	293	2019	64	38,34751	17	31,34199	2013,1	-1,4	-67,9	1943,9	570636,10	460594,84	K
K07-19	10,180	5	5	125	2019	64	29,10683	17	42,04160	1602,0	0,0	-67,7	1534,3	562465,58	443242,08	K
K07-19	18,088	20	10	293	2019	64	29,10693	17	42,04319	1599,4	-1,3	-67,7	1530,5	562464,31	443242,25	K
S01-19	15,683	5	5	125	2019	64	7,00169	17	49,96829	786,2	0,0	-66,8	719,4	556873,22	402053,49	K
S01-19	9,542	29	11	333	2019	64	7,00209	17	49,96812	779,9	-0,3	-66,8	712,7	556873,34	402054,23	K
S02-19	14,276	5	5	125	2019	64	12,15507	17	48,97843	1072,0	0,0	-67,0	1004,9	557497,72	411641,93	K
S02-19	14,298	21	10	294	2019	64	12,14156	17	48,98334	1066,1	0,0	-67,0	999,1	557494,21	411616,75	K
S04-19	13,457	5	5	125	2019	64	16,17352	17	48,20267	1227,5	0,0	-67,2	1160,3	557984,36	419118,78	K
S04-19	13,156	21	10	294	2019	64	16,15526	17	48,22144	1221,3	0,0	-67,2	1154,1	557969,85	419084,58	K
S05-19	18,790	4	5	124	2019	64	20,50045	17	33,99728	1521,4	0,0	-67,5	1453,9	569272,72	427394,85	K
S05-19	13,250	21	10	294	2019	64	20,49860	17	34,01431	1515,6	0,0	-67,5	1448,1	569259,09	427391,09	K

Ske02-19	13,536	4	5	124	2019	64	18,16054	17	9,18374	1276,2	0,0	-67,2	1209,0	589381,27	423567,66	K
Ske03-19	12,572	4	5	124	2019	64	17,79952	17	0,00289	1321,3	0,0	-67,2	1254,1	596805,13	423122,52	K
Ske04-19	11,759	4	5	124	2019	64	19,49781	16	54,51513	1435,6	0,0	-67,3	1368,3	601126,31	426419,49	K
Ske04-19	20,145	19	10	292	2019	64	19,47918	16	54,56231	1430,1	0,0	-67,3	1362,9	601089,45	426383,63	K
Ske05-19	10,965	4	5	124	2019	64	21,69918	16	51,02986	1503,5	0,0	-67,3	1436,1	603794,92	430601,50	K
Ske05-19	20,579	19	10	292	2019	64	21,68817	16	51,04436	1498,3	0,0	-67,3	1430,9	603783,95	430580,66	K
Skf00-19	17,562	30	4	120	2019	64	15,46256	15	54,07173	1019,0	0,0	-66,0	953,0	650171,41	420930,33	K
Skf00-19	21,451	22	10	295	2019	64	15,46398	15	54,06949	1013,5	-1,1	-66,0	946,4	650173,09	420933,05	K
Skf01-19	20,418	30	4	120	2019	64	18,00775	16	4,98593	1352,5	0,0	-66,6	1285,9	641144,51	425234,87	K
Skf01-19	14,574	18	10	291	2019	64	18,00510	16	4,97026	1346,5	0,0	-66,6	1279,8	641157,36	425230,53	K
T01-19	9,747	6	5	126	2019	64	20,06623	18	6,84164	846,1	0,0	-67,3	778,8	542831,11	426102,82	K
T01-19	13,810	29	11	333	2019	64	20,06663	18	6,84495	838,1	-0,2	-67,3	770,6	542828,43	426103,53	K
T01ve-19	8,201	6	5	126	2019	64	19,47049	18	5,26572	943,5	0,0	-67,3	876,3	544116,76	425014,10	K
T01ve-19	17,003	21	10	294	2019	64	19,47191	18	5,27054	938,2	0,0	-67,3	870,9	544112,83	425016,68	K
T01ve-20	12,377	29	11	333	2019	64	19,47374	18	4,55305	961,1	-2,2	-67,3	891,7	544691,05	425028,48	K
T02-19	20,821	5	5	125	2019	64	19,60098	18	3,99677	991,9	0,0	-67,3	924,6	545135,90	425271,46	K
T02-19	15,246	21	10	294	2019	64	19,60120	18	4,00576	985,8	0,0	-67,3	918,5	545128,65	425271,76	K
T03-19	20,057	5	5	125	2019	64	20,20311	17	58,58382	1138,3	0,0	-67,3	1071,0	549480,00	426457,60	K
T03-19	16,450	21	10	294	2019	64	20,20026	17	58,60292	1133,3	0,0	-67,3	1066,0	549464,69	426452,06	K
T04-19	12,201	5	5	125	2019	64	21,33259	17	51,51542	1290,2	0,0	-67,4	1222,9	555136,18	428653,35	K
T04-19	15,849	21	10	294	2019	64	21,32802	17	51,53287	1286,5	-1,2	-67,4	1217,9	555122,29	428644,61	K
T05-19	11,061	5	5	125	2019	64	22,26822	17	42,99368	1415,2	0,0	-67,5	1347,7	561960,76	430522,98	K
T05-19	14,570	21	10	294	2019	64	22,26478	17	43,00772	1411,3	-1,4	-67,5	1342,4	561949,60	430516,36	K
T05rorg	15,182	21	10	294	2019	64	22,25230	17	43,14253	1408,9	0,0	-67,5	1341,5	561841,61	430490,99	K
T05rorg	11,504	29	11	333	2019	64	22,25159	17	43,14515	1408,9	0,0	-67,5	1341,4	561839,53	430489,62	K
T05rorh	11,504	29	11	333	2019	64	22,25159	17	43,14515	1408,9	0,9	-67,5	1342,3	561839,53	430489,62	K
T06-19	9,583	5	5	125	2019	64	24,26747	17	36,50790	1538,3	0,0	-67,6	1470,7	567096,77	434347,11	K
T06-19	13,915	21	10	294	2019	64	24,26299	17	36,52040	1534,6	-1,7	-67,6	1465,3	567086,91	434338,56	K
T07-19	18,122	4	5	124	2019	64	25,29587	17	31,19732	1633,9	0,0	-67,7	1566,2	571319,03	436354,27	K
T07-19	18,950	20	10	293	2019	64	25,29385	17	31,20683	1630,5	-1,3	-67,7	1561,4	571311,48	436350,35	K
T08-19	17,679	4	5	124	2019	64	26,29197	17	27,75489	1706,9	0,0	-67,8	1639,2	574038,17	438270,47	K
T08-19	18,385	20	10	293	2019	64	26,29134	17	27,75727	1704,3	-1,5	-67,8	1635,0	574036,29	438269,25	K

Appendix D: Measured surface velocity at marked sites on Vatnajökull in 2019.

Site	Calendar day date	#	Calendar day date	#	# of days	translation (m)	(°)	velocity (cm/day)	(m/annum)
B07-19	190501	121	191018	291	170	1,69	168	0,99	3,62
B09-19	190503	123	191019	292	169	1,75	30	1,04	3,78
B10-19	190503	123	191019	292	169	0,72	297	0,43	1,56
B11-19	190503	123	191019	292	169	10,09	19	5,97	21,79
B12-19	190503	123	191019	292	169	27,86	21	16,48	60,17
B13ror15	181009	282	190503	123	206	10,46	29	5,08	18,54
B13ror15	190503	123	191019	292	169	37,05	28	21,92	80,01
B14-19	190503	123	191019	292	169	31,06	37	18,38	67,08
B15-19	190503	123	191019	292	169	17,49	46	10,35	37,77
B16-19	190530	150	191019	292	142	0,81	343	0,57	2,09
B17-19	190503	123	191019	292	169	32,93	17	19,49	71,13
B18-19	190501	121	191018	291	170	11,63	345	6,84	24,96
B19-19	190501	121	191018	291	170	0,85	322	0,50	1,83
BB0-19	190501	121	191018	291	170	1,43	259	0,84	3,08
Bor-19	190606	157	190830	241	84	6,76	207	8,05	29,39
Bor-19	190830	241	191022	295	54	7,77	183	14,39	52,52
Borth-17	181011	284	190305	64	145	0,48	279	0,33	1,21
Borth-19	190608	159	190830	241	82	6,89	185	8,41	30,69
Borth-19	190830	241	191022	295	54	3,31	172	6,13	22,36
Br1-19	190403	94	191127	331	237	1,15	230	0,49	1,78
Br2-18	180802	214	190403	94	245	4,07	155	1,66	6,07
Br2-19	190403	94	191127	331	237	3,06	176	1,29	4,72
Br3-19	190404	95	191128	332	237	17,06	143	7,20	26,28
Br4-18	180324	83	190404	95	377	336,58	181	89,28	325,86
Br5-19	190404	95	190501	121	26	25,61	183	98,49	359,47
Br7-19	190501	121	191018	291	170	50,60	174	29,77	108,65
Bru-19	190502	122	191019	292	170	17,84	11	10,49	38,30
Bud-19	190502	122	191018	291	169	22,70	5	13,43	49,02
D05-19	190504	124	191020	293	169	24,73	30	14,64	53,42
D06GPS19	190603	154	191020	293	139	20,92	30	15,05	54,93
D07-19	190504	124	191020	293	169	32,03	23	18,96	69,19
D09-19	190504	124	191020	293	169	7,40	348	4,38	15,99
D12-19	190504	124	191020	293	169	0,57	36	0,34	1,24
E01-19	190502	122	191019	292	170	5,79	20	3,40	12,43
E02-19	190502	122	191019	292	170	24,66	9	14,51	52,94
E03-19	190502	122	191019	292	170	10,08	346	5,93	21,64
E04-19	190501	121	191019	292	171	1,52	9	0,89	3,24
Fl01-19	190501	121	191018	291	170	17,51	137	10,30	37,59
G02-19	190602	153	191020	293	140	8,52	201	6,08	22,20
G03-19	190602	153	191020	293	140	4,21	201	3,01	10,99
G04-19	190602	153	191020	293	140	0,35	248	0,25	0,90
Go1-19	190601	152	191020	293	141	2,94	175	2,08	7,60
Haab-19	190606	157	191020	293	136	0,63	300	0,46	1,69
Hof01-19	190501	121	191019	292	171	11,36	179	6,64	24,24

K01-19	190505	125	191020	293	168	8,66	296	5,16	18,82
K02-19	190505	125	191020	293	168	14,76	297	8,79	32,07
K03-19	190505	125	191020	293	168	18,80	289	11,19	40,83
K04-19	190505	125	191020	293	168	22,48	289	13,38	48,84
K05-19	190505	125	191020	293	168	13,12	246	7,81	28,51
K06-19ve	190601	152	191020	293	141	2,15	159	1,52	5,56
K07-19	190505	125	191020	293	168	1,29	278	0,77	2,80
S01-19	190505	125	191129	333	208	0,75	11	0,36	1,32
S02-19	190505	125	191021	294	169	25,33	189	14,99	54,72
S04-19	190505	125	191021	294	169	37,06	204	21,93	80,04
S05-19	190504	124	191021	294	170	14,13	256	8,31	30,35
Ske04-19	190504	124	191019	292	168	51,34	228	30,56	111,53
Ske05-19	190504	124	191019	292	168	23,49	210	13,98	51,04
Skf00-19	190430	120	191022	295	175	3,19	35	1,82	6,66
Skf01-19	190430	120	191018	291	171	13,56	111	7,93	28,94
T01-19	190506	126	191129	333	207	2,77	286	1,34	4,88
T01ve-19	190506	126	191021	294	168	4,69	304	2,79	10,19
T02-19	190505	125	191021	294	169	7,25	273	4,29	15,67
T03-19	190505	125	191021	294	169	16,26	251	9,62	35,12
T04-19	190505	125	191021	294	169	16,40	239	9,70	35,41
T05-19	190505	125	191021	294	169	12,97	241	7,67	28,00
T05rorg	171026	299	191021	294	725	48,59	238	6,70	24,46
T05rorg	191021	294	191129	333	39	2,48	238	6,37	23,25
T06-19	190505	125	191021	294	169	13,03	230	7,71	28,13
T07-19	190504	124	191020	293	169	8,50	244	5,03	18,36
T08-19	190504	124	191020	293	169	2,24	239	1,32	4,83

Appendix E: Melt water runoff to selected rivers in summer 2019, derived from summer surface balance.

ΔS: area in a given elevation range where summer balance is negative, **∑ΔS**: cumulative area above a given elevation, **ΔQ_s**: melt water runoff from a given elevation range, **$\sum\Delta Q_s$** : cumulative melt water runoff from an area above given elevation.

Tungnaá water drainage basin

Elevation (m a. s. l.)		ΔS km^2	∑ΔS km^2	ΔQ_s $(10^6 m^3)$	$\sum\Delta Q_s$ $(10^6 m^3)$
1350	1400	0,4	0,4	1,0	1,0
1300	1350	6,1	6,4	17,9	18,9
1250	1300	10,2	16,7	32,3	51,2
1200	1250	10,9	27,6	36,4	87,5
1150	1200	9,9	37,5	35,6	123,2
1100	1150	11,9	49,4	45,3	168,5
1050	1100	11,9	61,4	47,6	216,1
1000	1050	9,6	71,0	40,6	256,7
950	1000	9,6	80,6	43,5	300,2
900	950	9,2	89,8	45,0	345,1
850	900	7,8	97,5	42,4	387,5
800	850	7,7	105,2	46,3	433,8
750	800	7,0	112,1	41,6	475,4
700	750	4,7	116,9	26,2	501,6
650	700	2,1	119,0	8,5	510,1

Sylgja water drainage basin

Elevation (m a. s. l.)		ΔS km^2	∑ΔS km^2	ΔQ_s $(10^6 m^3)$	$\sum\Delta Q_s$ $(10^6 m^3)$
1300	1350	1,1	1,1	3,5	3,5
1250	1300	3,6	4,7	11,4	14,9
1200	1250	5,9	10,5	19,7	34,6
1150	1200	8,3	18,8	29,2	63,8
1100	1150	6,1	24,9	22,7	86,5
1050	1100	6,9	31,8	27,1	113,6
1000	1050	5,1	36,9	21,4	135,0
950	1000	1,8	38,7	8,0	143,1
900	950	0,7	39,3	2,8	145,8
850	900	0,0	39,4	0,2	146,0

Western Skaftá cauldron water drainage basin

Elevation (m a. s. l.)		ΔS km^2	∑ΔS km^2	ΔQ_s $(10^6 m^3)$	$\sum\Delta Q_s$ $(10^6 m^3)$
1700	1750	2,5	2,5	2,5	2,5
1650	1700	7,2	9,7	8,0	10,4
1600	1650	8,5	18,2	10,7	21,2
1550	1600	5,4	23,6	7,2	28,4
1500	1550	1,5	25,1	2,0	30,4

Eastern Skaftár cauldron water drainage basin

Elevation (m a. s. l.)		ΔS km^2	∑ΔS km^2	ΔQ_s ($10^6 m^3$)	$\sum\Delta Q_s$ ($10^6 m^3$)
1750	1800	2,4	2,4	1,9	1,9
1700	1750	9,9	12,3	8,9	10,8
1650	1700	14,9	27,2	14,8	25,6
1600	1650	9,7	36,9	10,7	36,3
1550	1600	2,4	39,3	2,7	39,0

Grímsvötn water drainage basin

Elevation (m a. s. l.)		ΔS km^2	∑ΔS km^2	ΔQ_s ($10^6 m^3$)	$\sum\Delta Q_s$ ($10^6 m^3$)
1900	1950	0,4	0,4	0,3	0,3
1850	1900	1,3	1,8	0,9	1,2
1800	1850	1,7	3,4	1,2	2,4
1750	1800	4,3	7,7	3,5	6,0
1700	1750	18,6	26,3	16,4	22,3
1650	1700	53,3	79,6	52,4	74,7
1600	1650	30,9	110,4	36,1	110,8
1550	1600	19,3	129,7	24,3	135,1
1500	1550	16,8	146,4	23,8	158,9
1450	1500	10,0	156,5	17,2	176,1
1400	1450	11,7	168,2	24,6	200,6
1350	1400	4,3	172,5	9,2	209,9
1300	1350	0,7	173,2	1,5	211,4

Kaldakvísl water drainage basin

Elevation (m a. s. l.)		ΔS km^2	∑ΔS km^2	ΔQ_s ($10^6 m^3$)	$\sum\Delta Q_s$ ($10^6 m^3$)
1950	2000	1,7	1,7	1,0	1,0
1900	1950	14,7	16,4	9,1	10,1
1850	1900	6,9	23,4	5,1	15,3
1800	1850	6,5	29,8	5,3	20,6
1750	1800	11,4	41,2	9,5	30,1
1700	1750	20,2	61,5	19,9	50,0
1650	1700	17,1	78,5	21,5	71,5
1600	1650	14,5	93,0	21,1	92,6
1550	1600	19,1	112,1	31,3	123,9
1500	1550	25,2	137,3	45,6	169,5
1450	1500	28,8	166,1	57,0	226,6
1400	1450	24,0	190,1	53,9	280,5
1350	1400	22,1	212,2	58,6	339,1
1300	1350	21,2	233,4	65,0	404,1
1250	1300	22,4	255,9	80,3	484,4
1200	1250	21,7	277,5	90,5	574,9
1150	1200	20,0	297,5	94,1	669,0
1100	1150	18,0	315,5	91,9	760,9
1050	1100	16,9	332,3	89,9	850,8
1000	1050	14,6	346,9	81,6	932,4
950	1000	10,4	357,4	59,5	992,0
900	950	6,3	363,7	27,8	1019,7
850	900	0,9	364,6	2,7	1022,4

Jökulsá á Fjöllum water drainage basin

Elevation (m a. s. l.)		ΔS km^2	∑ΔS km^2	ΔQ_s ($10^6 m^3$)	$\sum\Delta Q_s$ ($10^6 m^3$)
1950	2000	3,7	3,7	2,5	2,5
1900	1950	15,4	19,2	9,7	12,2
1850	1900	28,3	47,4	20,4	32,6
1800	1850	20,0	67,4	15,3	47,9
1750	1800	22,0	89,4	18,4	66,3
1700	1750	34,7	124,1	30,9	97,1
1650	1700	80,2	204,3	75,1	172,2
1600	1650	120,9	325,2	129,4	301,7
1550	1600	100,3	425,5	123,5	425,1
1500	1550	93,4	518,9	128,3	553,4
1450	1500	80,6	599,5	123,2	676,6
1400	1450	69,8	669,3	121,1	797,7
1350	1400	56,3	725,6	112,9	910,5
1300	1350	43,3	768,9	99,9	1010,4
1250	1300	47,2	816,1	123,2	1133,6
1200	1250	51,6	867,7	151,1	1284,8
1150	1200	51,4	919,1	170,2	1455,0
1100	1150	44,8	963,9	166,9	1621,9
1050	1100	32,3	996,2	131,2	1753,1
1000	1050	33,5	1029,7	144,7	1897,8
950	1000	31,0	1060,6	144,6	2042,5
900	950	26,0	1086,6	131,2	2173,7
850	900	23,7	1110,4	126,9	2300,6
800	850	21,6	1131,9	114,4	2414,9
750	800	17,8	1149,7	86,0	2501,0
700	750	5,4	1155,1	20,9	2521,9

Kreppa and Kverká water drainage basin

Elevation (m a. s. l.)		ΔS km^2	$\sum\Delta S$ km^2	ΔQ_s $(10^6 m^3)$	$\sum\Delta Q_s$ $(10^6 m^3)$
1850	1900	1,3	1,4	0,9	0,9
1800	1850	4,4	5,8	2,3	3,2
1750	1800	2,7	8,5	1,6	4,8
1700	1750	3,8	12,3	2,8	7,6
1650	1700	5,2	17,5	4,2	11,8
1600	1650	41,4	58,9	43,7	55,5
1550	1600	20,5	79,4	22,8	78,3
1500	1550	13,4	92,8	16,6	94,9
1450	1500	16,3	109,1	22,0	116,9
1400	1450	19,8	128,9	28,9	145,8
1350	1400	25,5	154,4	40,6	186,4
1300	1350	20,0	174,4	35,1	221,5
1250	1300	15,5	189,9	29,7	251,2
1200	1250	17,7	207,6	36,7	287,9
1150	1200	17,7	225,3	38,8	326,7
1100	1150	16,9	242,2	39,7	366,4
1050	1100	11,1	253,3	29,3	395,7
1000	1050	13,4	266,7	39,7	435,4
950	1000	15,1	281,8	50,9	486,3
900	950	13,5	295,3	51,9	538,2
850	900	14,2	309,5	60,4	598,6
800	850	11,0	320,5	48,6	647,2
750	800	10,5	331,0	49,8	697,0
700	750	4,8	335,8	24,7	721,7
650	700	1,8	337,6	7,4	729,1

Hálslón water drainage basin

Elevation (m a. s. l.)		ΔS km^2	$\sum\Delta S$ km^2	ΔQ_s $(10^6 m^3)$	$\sum\Delta Q_s$ $(10^6 m^3)$
1600	1650	11,2	11,2	12,6	12,6
1550	1600	31,8	43,0	37,0	49,6
1500	1550	63,6	106,7	77,1	126,7
1450	1500	67,6	174,3	88,4	215,1
1400	1450	97,7	272,0	132,3	347,5
1350	1400	131,7	403,7	187,7	535,2
1300	1350	129,4	533,1	199,9	735,1
1250	1300	126,1	659,2	216,9	952,0
1200	1250	99,2	758,4	188,3	1140,2
1150	1200	84,7	843,1	178,0	1318,2
1100	1150	66,5	909,6	155,5	1473,7
1050	1100	58,7	968,3	151,6	1625,2
1000	1050	49,4	1017,7	142,6	1767,8
950	1000	41,4	1059,2	135,0	1902,8
900	950	32,9	1092,0	120,7	2023,5
850	900	28,5	1120,5	117,0	2140,5
800	850	27,2	1147,7	124,4	2264,9
750	800	26,6	1174,3	138,7	2403,6
700	750	20,8	1195,1	117,6	2521,2
650	700	15,7	1210,7	74,6	2595,8
600	650	3,0	1213,7	12,9	2608,7

Jökulsá á Fljótsdal water drainage basin

Elevation (m a. s. l.)		ΔS km^2	ΣΔS km^2	ΔQ_s ($10^6 m^3$)	$\Sigma\Delta Q_s$ ($10^6 m^3$)
1500	1550	0,0	0,0	0,1	0,1
1450	1500	0,9	1,0	1,1	1,2
1400	1450	1,9	2,9	2,4	3,6
1350	1400	2,8	5,8	4,0	7,6
1300	1350	5,4	11,2	8,6	16,2
1250	1300	16,2	27,4	28,0	44,2
1200	1250	16,0	43,4	30,6	74,8
1150	1200	17,3	60,7	36,1	110,9
1100	1150	15,0	75,7	35,2	146,1
1050	1100	12,4	88,1	33,1	179,1
1000	1050	11,9	100,0	35,0	214,1
950	1000	8,8	108,8	28,5	242,6
900	950	5,5	114,3	19,9	262,5
850	900	4,4	118,7	17,3	279,8
800	850	3,2	121,9	13,8	293,6
750	800	3,0	124,9	14,3	307,9
700	750	2,6	127,5	13,4	321,3
650	700	3,0	130,6	13,7	335,0
600	650	0,2	130,7	0,7	335,7

Hornafjarðarfljót water drainage basin

Elevation (m a. s. l.)		ΔS km^2	∑ΔS km^2	ΔQ_s ($10^6 m^3$)	$\sum\Delta Q_s$ ($10^6 m^3$)
1450	1500	1,0	1,0	1,2	1,2
1400	1450	8,2	9,2	10,1	11,2
1350	1400	12,7	21,8	17,0	28,2
1300	1350	19,1	40,9	30,4	58,6
1250	1300	37,9	78,9	68,6	127,2
1200	1250	29,1	108,0	59,2	186,4
1150	1200	20,5	128,4	48,1	234,5
1100	1150	19,1	147,5	51,1	285,6
1050	1100	14,5	162,0	45,1	330,7
1000	1050	11,4	173,4	40,0	370,7
950	1000	10,7	184,2	41,6	412,3
900	950	8,2	192,3	34,6	446,9
850	900	5,5	197,8	25,1	471,9
800	850	4,4	202,2	20,4	492,3
750	800	4,2	206,3	20,6	512,9
700	750	3,7	210,1	19,5	532,4
650	700	3,6	213,6	19,7	552,2
600	650	2,6	216,3	15,6	567,7
550	600	1,9	218,2	11,7	579,5
500	550	1,9	220,1	12,1	591,6
450	500	1,3	221,4	8,5	600,1
400	450	1,3	222,7	9,3	609,4
350	400	0,8	223,6	6,0	615,4
300	350	0,9	224,5	6,6	622,0
250	300	1,5	225,9	11,1	633,1
200	250	2,9	228,8	23,0	656,1
150	200	3,1	232,0	30,0	686,1
100	150	2,4	234,4	24,9	711,0
50	100	1,8	236,2	18,9	729,9
0	50	2,6	238,9	23,3	753,3

Jökulsá á Breiðamerkursandi water drainage basin

Elevation (m a. s. l.)		ΔS km^2	∑ΔS km^2	ΔQ_s ($10^6 m^3$)	$\sum\Delta Q_s$ ($10^6 m^3$)
1700	1750	1,0	1,0	0,9	0,9
1650	1700	4,2	5,2	4,0	4,9
1600	1650	13,8	19,0	13,7	18,6
1550	1600	19,0	38,0	20,6	39,2
1500	1550	23,2	61,2	29,8	68,9
1450	1500	36,2	97,4	50,6	119,5
1400	1450	51,2	148,6	76,4	195,9
1350	1400	84,2	232,8	136,2	332,1
1300	1350	83,4	316,2	148,2	480,4
1250	1300	51,6	367,9	103,8	584,1
1200	1250	35,1	403,0	79,7	663,8
1150	1200	28,2	431,2	72,2	736,0
1100	1150	24,1	455,3	70,7	806,7
1050	1100	20,5	475,7	67,2	873,9
1000	1050	17,6	493,3	63,1	937,0
950	1000	18,9	512,2	72,9	1009,9
900	950	20,0	532,3	80,9	1090,7
850	900	19,9	552,2	86,5	1177,2
800	850	20,1	572,3	93,5	1270,8
750	800	19,5	591,9	98,5	1369,2
700	750	19,2	611,1	101,9	1471,2
650	700	27,6	638,7	150,3	1621,4
600	650	18,4	657,1	108,1	1729,5
550	600	18,7	675,8	117,2	1846,7
500	550	7,6	683,3	49,4	1896,1
450	500	6,5	689,8	45,1	1941,2
400	450	6,4	696,2	45,6	1986,8
350	400	5,3	701,4	38,2	2025,0
300	350	5,7	707,1	42,3	2067,3
250	300	5,5	712,6	42,1	2109,4
200	250	5,9	718,5	48,3	2157,7
150	200	5,3	723,8	53,6	2211,3
100	150	4,9	728,7	54,9	2266,2
50	100	4,8	733,5	45,2	2311,4
0	50	3,9	737,4	28,5	2339,9

Breiðárlón/Fjallsárlón water drainage basin

Elevation (m a. s. l.)		ΔS km^2	∑ΔS km^2	ΔQ_s ($10^6 m^3$)	$\sum\Delta Q_s$ ($10^6 m^3$)
2000	2050	0,1	0,1	0,0	0,0
1950	2000	0,6	0,8	0,2	0,2
1900	1950	1,0	1,7	0,3	0,6
1850	1900	1,6	3,4	0,6	1,2
1800	1850	2,1	5,5	1,0	2,2
1750	1800	2,7	8,2	1,5	3,7
1700	1750	2,9	11,1	2,2	5,9
1650	1700	3,0	14,1	2,6	8,5
1600	1650	4,2	18,3	4,8	13,3
1550	1600	4,3	22,6	5,6	18,9
1500	1550	5,7	28,3	8,3	27,2
1450	1500	4,9	33,3	8,1	35,3
1400	1450	5,3	38,6	10,0	45,3
1350	1400	6,3	44,9	13,8	59,1
1300	1350	12,6	57,5	30,6	89,7
1250	1300	6,5	64,0	16,6	106,3
1200	1250	5,6	69,6	15,3	121,7
1150	1200	4,9	74,5	14,1	135,7
1100	1150	4,5	78,9	14,0	149,7
1050	1100	5,0	83,9	16,5	166,2
1000	1050	6,0	89,9	20,8	187,0
950	1000	6,9	96,8	26,6	213,5
900	950	8,3	105,0	33,9	247,4
850	900	6,6	111,7	29,1	276,5
800	850	8,1	119,8	38,4	315,0
750	800	8,7	128,5	44,9	359,9
700	750	6,2	134,7	33,7	393,6
650	700	7,1	141,8	40,1	433,7
600	650	7,9	149,6	46,8	480,5
550	600	8,6	158,3	54,2	534,7
500	550	8,7	166,9	56,7	591,4
450	500	9,1	176,0	61,8	653,2
400	450	11,0	187,0	77,9	731,1
350	400	8,9	195,9	65,2	796,4
300	350	6,9	202,7	51,1	847,4
250	300	6,9	209,6	52,6	900,0
200	250	7,1	216,7	57,4	957,4
150	200	5,3	222,0	50,5	1007,9
100	150	4,3	226,4	46,1	1054,1
50	100	4,1	230,4	41,9	1096,0
0	50	3,3	233,7	30,5	1126,5

Skeiðarársandur (Gígja without Súla) water drainage basin

Elevation (m a. s. l.)		ΔS km^2	∑ΔS km^2	ΔQ_s ($10^6 m^3$)	$\sum\Delta Q_s$ ($10^6 m^3$)
1700	1750	1,9	1,9	2,1	2,1
1650	1700	21,2	23,1	23,1	25,2
1600	1650	83,4	106,5	92,0	117,2
1550	1600	86,0	192,5	102,5	219,7
1500	1550	111,4	303,9	145,5	365,2
1450	1500	107,4	411,3	164,4	529,6
1400	1450	103,7	515,0	183,0	712,6
1350	1400	90,8	605,8	177,0	889,6
1300	1350	78,1	683,9	165,2	1054,8
1250	1300	69,5	753,4	157,9	1212,7
1200	1250	60,4	813,8	146,7	1359,4
1150	1200	53,6	867,4	141,8	1501,2
1100	1150	52,4	919,8	147,6	1648,8
1050	1100	46,5	966,3	142,2	1791,0
1000	1050	41,3	1007,6	138,0	1929,0
950	1000	41,1	1048,7	150,7	2079,7
900	950	38,8	1087,5	157,0	2236,7
850	900	39,8	1127,3	180,4	2417,1
800	850	33,1	1160,4	170,5	2587,6
750	800	26,0	1186,4	148,8	2736,4
700	750	26,0	1212,4	158,8	2895,2
650	700	19,3	1231,7	124,3	3019,5
600	650	17,2	1248,9	114,6	3134,1
550	600	25,0	1273,9	170,4	3304,5
500	550	19,9	1293,8	136,7	3441,2
450	500	13,6	1307,4	94,7	3535,9
400	450	13,1	1320,5	94,4	3630,3
350	400	14,3	1334,8	111,3	3741,6
300	350	15,0	1349,8	131,1	3872,7
250	300	13,7	1363,5	130,6	4003,3
200	250	13,4	1376,9	135,1	4138,4
150	200	11,2	1388,1	118,5	4256,9
100	150	9,6	1397,7	97,3	4354,2
50	100	8,6	1406,3	71,2	4425,4
0	50	0,2	1406,5	1,2	4426,6

Súla water drainage basin

Elevation (m a. s. l.)		ΔS km^2	∑ΔS km^2	ΔQ$_s$ (10^{6}m^3)	∑ΔQ$_s$ (10^{6}m^3)
1700	1750	0,5	0,5	0,7	0,7
1650	1700	1,5	2,0	1,8	2,5
1600	1650	2,5	4,5	3,3	5,8
1550	1600	4,0	8,6	5,7	11,5
1500	1550	5,9	14,4	9,0	20,6
1450	1500	11,1	25,5	19,8	40,4
1400	1450	11,0	36,5	21,5	61,8
1350	1400	9,3	45,8	19,4	81,3
1300	1350	8,2	54,0	17,7	99,0
1250	1300	6,6	60,5	14,9	113,9
1200	1250	7,9	68,5	18,6	132,5
1150	1200	8,8	77,3	21,8	154,4
1100	1150	15,2	92,4	40,2	194,5
1050	1100	16,0	108,4	46,6	241,2
1000	1050	16,7	125,1	54,5	295,7
950	1000	18,0	143,1	65,8	361,5
900	950	15,4	158,5	62,3	423,8
850	900	11,4	169,8	51,0	474,8
800	850	11,9	181,7	60,3	535,1
750	800	7,4	189,1	42,5	577,5
700	750	5,9	195,0	36,6	614,2
650	700	5,1	200,1	32,6	646,8
600	650	5,6	205,7	37,4	684,2
550	600	11,1	216,8	75,8	760,0
500	550	10,5	227,3	72,2	832,2
450	500	7,3	234,5	50,8	883,0
400	450	6,5	241,0	46,7	929,7
350	400	5,1	246,1	39,2	968,9
300	350	2,7	248,8	23,6	992,4
250	300	1,0	249,8	10,1	1002,5
200	250	0,8	250,6	8,4	1010,9
150	200	0,7	251,3	7,2	1018,1
100	150	0,7	252,0	7,6	1025,8
50	100	0,7	252,8	7,3	1033,0

Djúpá water drainage basin

Elevation (m a. s. l.)		ΔS km^2	∑ΔS km^2	ΔQ$_s$ (10^{6}m^3)	∑ΔQ$_s$ (10^{6}m^3)
1450	1500	0,0	0,0	0,2	0,2
1400	1450	0,3	0,4	0,8	1,1
1350	1400	0,7	1,1	2,0	3,0
1300	1350	3,5	4,6	10,7	13,7
1250	1300	3,4	8,0	10,9	24,6
1200	1250	3,0	11,0	10,5	35,1
1150	1200	3,5	14,5	13,1	48,2
1100	1150	5,3	19,9	20,4	68,6
1050	1100	6,1	26,0	24,8	93,4
1000	1050	9,2	35,2	40,7	134,1
950	1000	7,3	42,4	35,4	169,6
900	950	7,8	50,2	39,4	209,0
850	900	6,7	56,9	34,5	243,5
800	850	8,0	64,8	42,6	286,1
750	800	6,6	71,4	36,0	322,1
700	750	3,7	75,1	22,7	344,8
650	700	2,9	78,0	17,2	362,0
600	650	1,0	79,0	4,6	366,7

Brunná water drainage basin

Elevation (m a. s. l.)		ΔS km^2	∑ΔS km^2	ΔQ$_s$ (10^{6}m^3)	∑ΔQ$_s$ (10^{6}m^3)
1050	1100	0,0	0,0	0,0	0,0
1000	1050	0,9	1,0	4,5	4,5
950	1000	2,5	3,5	12,5	17,0
900	950	4,3	7,8	22,1	39,1
850	900	4,2	12,0	22,1	61,2
800	850	4,2	16,2	22,9	84,1
750	800	4,6	20,7	26,9	111,1
700	750	5,6	26,4	35,9	146,9
650	700	4,8	31,2	32,8	179,7
600	650	3,2	34,4	15,7	195,5
550	600	0,5	34,9	2,3	197,8

Hverfisfljót water drainage basin

Elevation (m a. s. l.)		ΔS km^2	∑ΔS km^2	ΔQ_s ($10^6 m^3$)	$\sum\Delta Q_s$ ($10^6 m^3$)
1700	1750	0,9	0,9	1,1	1,1
1650	1700	5,5	6,4	6,6	7,7
1600	1650	9,1	15,5	11,1	18,8
1550	1600	9,6	25,1	12,3	31,1
1500	1550	19,9	45,0	26,4	57,5
1450	1500	41,1	86,1	67,8	125,3
1400	1450	27,6	113,7	57,0	182,3
1350	1400	24,1	137,8	60,3	242,5
1300	1350	22,8	160,6	64,8	307,3
1250	1300	18,1	178,7	56,8	364,1
1200	1250	20,2	198,9	69,1	433,1
1150	1200	14,6	213,5	54,8	488,0
1100	1150	11,1	224,6	43,1	531,1
1050	1100	9,6	234,1	38,9	570,0
1000	1050	9,0	243,1	41,2	611,3
950	1000	8,9	252,0	43,9	655,2
900	950	8,6	260,5	43,9	699,0
850	900	7,8	268,3	41,1	740,1
800	850	7,3	275,5	40,3	780,3
750	800	10,1	285,6	60,2	840,5
700	750	12,1	297,7	78,6	919,1
650	700	10,5	308,2	72,1	991,2
600	650	6,2	314,4	35,6	1026,8
550	600	1,0	315,4	4,7	1031,5

Skaftá water drainage basin

Elevation (m a. s. l.)		ΔS km^2	∑ΔS km^2	ΔQ_s ($10^6 m^3$)	$\sum\Delta Q_s$ ($10^6 m^3$)
1650	1700	2,2	2,2	2,4	2,4
1600	1650	15,6	17,8	18,6	21,0
1550	1600	22,7	40,4	29,6	50,6
1500	1550	30,8	71,2	41,9	92,5
1450	1500	24,5	95,7	36,4	128,9
1400	1450	22,3	118,0	43,8	172,7
1350	1400	20,5	138,5	50,9	223,6
1300	1350	22,5	161,0	64,7	288,3
1250	1300	15,6	176,6	49,0	337,3
1200	1250	21,0	197,6	71,6	408,9
1150	1200	22,7	220,2	83,7	492,6
1100	1150	23,7	243,9	91,2	583,8
1050	1100	24,2	268,1	95,7	679,5
1000	1050	26,2	294,3	113,4	792,9
950	1000	20,6	314,9	98,6	891,5
900	950	16,7	331,7	86,4	978,0
850	900	14,4	346,0	79,0	1057,0
800	850	14,8	360,8	86,4	1143,4
750	800	12,3	373,1	76,3	1219,8
700	750	9,7	382,8	62,1	1281,9
650	700	5,8	388,6	33,1	1315,0
600	650	1,1	389,7	5,1	1320,1